PB82-115528

Control of Particulate Emissions from Atmospheric Fluidized-Bed Combustion with Fabric Filters and Electrostatic Precipitators

GCA Corp.
Bedford, MA

Prepared for

Industrial Environmental Research Lab.
Research Triangle Park, NC

Jun 81

U.S. Department of Commerce
National Technical Information Service
NTIS

PB82-115528

EPA-600/7-81-105
June 1981

Sponsored by

U.S. ENVIRONMENTAL PROTECTION AGENCY
OFFICE OF RESEARCH AND DEVELOPMENT
Washington, D.C. 20460

Contract No. 68-02-2693

EPA Project Officer: J. O. Milliken

INDUSTRIAL ENVIRONMENTAL RESEARCH LABORATORY
OFFICE OF ENVIRONMENTAL ENGINEERING AND TECHNOLOGY
Research Triangle Park, North Carolina 27711

CONTROL OF PARTICULATE EMISSIONS FROM ATMOSPHERIC FLUIDIZED-BED COMBUSTION WITH FABRIC FILTERS AND ELECTROSTATIC PRECIPITATORS

Prepared by

David V. Bubenick
Robert R. Hall
John A. Dirgo

GCA CORPORATION
GCA/TECHNOLOGY DIVISION
Bedford, Massachusetts
01730

REPRODUCED BY
NATIONAL TECHNICAL
INFORMATION SERVICE
U.S. DEPARTMENT OF COMMERCE
SPRINGFIELD, VA 22161

NOTICE

THIS DOCUMENT HAS BEEN REPRODUCED FROM THE BEST COPY FURNISHED US BY THE SPONSORING AGENCY. ALTHOUGH IT IS RECOGNIZED THAT CERTAIN PORTIONS ARE ILLEGIBLE, IT IS BEING RELEASED IN THE INTEREST OF MAKING AVAILABLE AS MUCH INFORMATION AS POSSIBLE.

TECHNICAL REPORT DATA (Please read Instructions on the reverse before completing)		
1. REPORT NO. EPA-600/7-81-105	2.	3. RECIPIENT'S ACCESSION NO. PB82 115528
4. TITLE AND SUBTITLE Control of Particulate Emissions from Atmospheric Fluidized-bed Combustion with Fabric Filters and Electrostatic Precipitators		5. REPORT DATE June 1981 6. PERFORMING ORGANIZATION CODE
7. AUTHOR(S) D. V. Bubenick, R. R. Hall, and J. A. Dirgo		8. PERFORMING ORGANIZATION REPORT NO.
9. PERFORMING ORGANIZATION NAME AND ADDRESS GCA/Technology Division 213 Burlington Road Bedford, Massachusetts 01730		10. PROGRAM ELEMENT NO. CCZN1A 11. CONTRACT/GRANT NO. 68-02-2693
12. SPONSORING AGENCY NAME AND ADDRESS EPA, Office of Research and Development Industrial Environmental Research Laboratory Research Triangle Park, NC 27711		13. TYPE OF REPORT AND PERIOD COVERED Final; 12/79 - 12/80 14. SPONSORING AGENCY CODE EPA/600/13
15. SUPPLEMENTARY NOTES IERL-RTP project officer is John O. Milliken, Mail Drop 61, 919/541-7716.		

16. ABSTRACT The report gives results of a study of chemical and physical characteristics affecting the performance of particulate control equipment, based on five fly ash samples from full- and pilot-scale atmospheric fluidized-bed combustion (AFBC) units. Analysis of acquired data by fabric filter (FF) and electrostatic precipitator (ESP) mathematical models illustrates how control device performance may be affected by AFBC fly ash properties. Laboratory measurements of the specific resistance coefficient (K2), a measure of the pressure loss through a dust deposit on a fabric, ranged from 1.9 to 5.3 N-min/g-m for the AFBC fly ashes, compared to values near 2.0 N-min/g-m for conventional fly ash. Mathematical simulation of an operating FF indicated that an increase in K2 from 2 to 5 N-min/g-m could result in a 30% increase in penetration and a doubling of pressure loss. Low electrical resistivity values (100,000 to 10 million ohm-cm) of two fly ash samples containing high carbon (34-46%) would probably cause poor ESP performance. The remaining three samples exhibited resistivities falling within the range of conventional combustion design experience with ESPs. Efficient operation of mechanical precollectors or combustion efficiency improvements would reduce the impact of high carbon carryover, thereby minimizing FF fabric blinding and ESP sparkover.

17. KEY WORDS AND DOCUMENT ANALYSIS

a. DESCRIPTORS		b. IDENTIFIERS/OPEN ENDED TERMS	c. COSATI Field/Group	
Pollution	Aerosols	Pollution Control	13B	07D
Fluidized Bed Processing	Filtration	Stationary Sources		
Combustion	Fabrics	Particulate	13H,07A	11E
Coal	Electrostatic Precipitators	Fabric Filters	21B	
Fly Ash			21D	13I
Dust			11G	

18. DISTRIBUTION STATEMENT	19. SECURITY CLASS (This Report)	21. NO. OF PAGES
Release to Public	Unclassified	77
	20. SECURITY CLASS (This page) Unclassified	22. PRICE

EPA Form 2220-1 (9-73)

DISCLAIMER

This report has been reviewed by the Industrial Environmental Research Laboratory (RTP), U.S. Environmental Protection Agency, and approved for publication. Approval does not signify that the contents necessarily reflect the views and policies of the Agency, nor does mention of trade names or commercial products constitute endorsement or recommendation for use.

COLOR ILLUSTRATIONS REPRODUCED
IN BLACK AND WHITE

ABSTRACT

Fabric filters are being installed on many new atmospheric fluidized-bed combustion (AFBC) units, despite the lack of test or demonstration data. For this reason, the present study focuses on assessing fundamental chemical and physical characteristics affecting the performance of particulate control equipment based on five fly ash samples from full- and pilot-scale AFBC units. These results were used in conjunction with fabric filter (FF) and electrostatic precipitator (ESP) mathematical models to illustrate how control device performance may be affected by AFBC fly ash properties. Laboratory measurements of the specific resistance coefficient (K_2), a measure of the pressure loss through a dust deposit on a fabric, ranged from 1.9 to 5.3 N-min/g-m for the AFBC fly ashes, compared to values near 2.0 N-min/g-m for conventional fly ash. Mathematical simulation of an operating FF indicated that an increase in K_2 from 2 to 5 N-min/g-m could result in a 30 percent increase in penetration and a doubling of pressure loss. Low electrical resistivity values (10^5 to 10^7 ohm-cm) of two fly ash samples containing high carbon (34 to 46 percent) would be expected to cause poor ESP performance. The remaining three samples exhibited resistivities falling within the range of conventional combustion design experience with ESPs as shown by model simulation. Efficient operation of the mechanical precollectors or combustion efficiency improvements may reduce the impact of high carbon carryover and thereby minimize possible fabric blinding for FFs and sparkover resulting in poor ESP performance. The ultimate choice of a particulate control device must take into account all of the above factors as well as case-by-case and transient AFBC operating conditions.

CONTENTS

Abstract iii
Figures v
Tables vi
Acknowledgments vii

1. Introduction 1
   AFBC Installations 1
   Fabric Filter Installations 3
   Electrostatic Precipitator Installations 5
2. Approach 6
   Fabric Filter Model 9
   Electrostatic Precipitator Model 10
3. Results/Discussion 12
   Fabric Filter Analysis 14
   Electrostatic Precipitator Analysis 18
   Field Operating Considerations 25
4. Summary/Future Work 27

References 29
Appendices

A. Particle Size and Filtration Parameter Measurements 31
B. Resistivity Measurements 47
C. Morphology Characterization and Chemical/Spectral Analysis 57

FIGURES

Number		Page
1	Representative morphology for FBC fly ash	15
2	Representative morphology for conventional coal-fired boiler fly ash	15
3	The effect of air-to-cloth ratio on particle penetration for different K_2 levels	16
4	The effect of air-to-cloth ratio on filter pressure drop for different K_2 levels	17
5	Penetration and filter pressure drop as a function of fraction of filter area cleaned	19
6	Summary of resistivity data	20
7	Effect of fly ash resistivity on cold ESP overall mass collection efficiency as a function of specific collection area	22
8	Summary of fly ash particle size distributions	23
9	Effect of particle size distribution on cold ESP overall mass collection efficiency as a function of specific collection area	24

TABLES

Number		Page
1	Operating Conditions for AFBCs Equipped with Fabric Filters . . .	2
2	Fabric Filters Planned and Operating on Atmospheric Fluidized-Bed Combustion Units--U.S.	4
3	FBC Operating Conditions for Fly Ash Samples	7
4	Summary of FBC Fly Ash Measurements	8
5	Results of Fundamental Measurements Performed on FBC Fly Ash Samples	13

ACKNOWLEDGMENTS

The authors express their appreciation to D. Bruce Henschel, who was the EPA Project Officer during the performance of this taskwork, for his technical support and guidance throughout the program. Our thanks are also extended to the Health Effects Research Laboratory of EPA at Research Triangle Park, North Carolina for providing the photomicrographs used in Figures 1 and 2. Finally, the authors wish to acknowledge the work of Hans A. Klemm and David C. Lee of GCA/Technology Division who provided assistance in fabric filter computer analysis and electrostatic precipitator computer analysis, respectively.

SECTION 1

INTRODUCTION

In June of 1978, the U.S. Environmental Protection Agency awarded a 4-year contract to GCA/Technology Division to perform a comprehensive environmental assessment and systems analysis of fluidized-bed combustion technology. The ultimate objective of this program is to ensure that an adequate research data base is available to EPA Program Offices as they develop or revise pollution standards in conjunction with a national energy policy. As part of the engineering assessment of control technology for atmospheric fluidized-bed combustion (AFBC), GCA is investigating the suitability of fabric filters and electrostatic precipitators (ESPs) as final particulate collectors.

Initial efforts were directed at examining selected planned and operating fabric filters and electrostatic precipitators applied to AFBC boilers. This survey led to the conclusion that fabric filters are being installed on virtually all new AFBC units despite the lack of comprehensive test or demonstration data. ESPs, on the other hand, have been applied on a rather limited basis. With this lack of a working data base, a more fundamental approach was elected to assess particulate control device suitability. This consisted of first making basic measurements on selected fly ash samples obtained from operating pilot and full-scale AFBCs in the United States. Then, with the aid of analytical mathematical performance models, which are available for fabric filters and ESPs, basic relationships among key design and performance parameters were examined. Both the results of measurements made and relationships examined are presented in this report along with an assessment of additional data needs, stressing the importance of laboratory and field verification of control device performance.

AFBC INSTALLATIONS

Although there are basic design similarities with respect to key parameters among the AFBCs (full scale and experimental) equipped with fabric filters, manufacturers' designs can differ considerably, as shown in Table 1. Fluidizing velocities, for example, typically fall in the range of 2.1 to 2.4 m/sec (7 to 8 ft/sec), although depending on bed geometry, freeboard height, and Ca/S ratio, they may range from 0.9 to 4.9 m/sec (3 to 16 ft/sec). The type of coal feeding also varies according to manufacturers' design, from overbed feeding (used only at the Georgetown facility) to underbed feeding, with inbed feeding used at some sites. The above parameters and other factors, such as sorbent attrition, coal and sorbent characteristics, and the extent of fly ash recycle can affect the quantity and characteristics of

TABLE 1. OPERATING CONDITIONS FOR AFBCs EQUIPPED WITH FABRIC FILTERS

	Georgetown University, Washington, D.C.	Central Ohio Psychiatric Hospital, Ohio	Great Lakes Naval Training Center, Ill.	Pope, Evans, and Robbins Demonstration Unit, Alexandria, Va.	Combustion Engineering Demonstration Unit, Windsor, Conn.	FluiDyne Engineering Demonstration Unit, Minneapolis, Minn.	EPRI/B&W* Pilot Plant, Alliance, Ohio	SATR† Experimental Unit, EPA, Research Triangle Park, N.C.	Grand Forks Energy Research Center Experimental Unit, Grand Forks, N.D.
Coal feed rate (kg/hr)	4340-4350	2800	2750	280-360	70-160	70-235	840-885	9-50	91
Feeder type	Overbed	Underbed	Underbed	Variable	Underbed	Inbed	Underbed	Underbed	Inbed
Calcium-to-sulfur ratio (mole/mole)	3-5	2-4	3-4	Variable	2-4	1.1-2.8	2.4-4	2.5-3	2-3.5
Bed cross-sectional area (m^2)	20	-	13	0.84	0.8	1.6	3.3	0.14	0.2
Freeboard height (m)	2.4	-	1.8	-	-	-	6.0	3.0	2.5
Bed temperature (^oC)	840-870	850	850	750-900	850	790-900	840	750-1110	850-925
Fluidizing velocity (m/sec)	1.75-2.5	2.4	2.1	3.4-3.7	1.5-2.7	0.9-2.1	2.4	0.9-4.9	1-4
Flue gas temperature (^oC)	180-230	205-230	175-230	205-230	150-175	180-195	190-205	175-230	120-175

*Electric Power Research Institute/Babcock & Wilcox.

†Sampling and Analytical Test Rig, presently not operating.

particulate emissions from AFBC units. Later in this report, the importance of the mechanical precollectors or cyclones will be discussed insofar as they reduce particulate loading and carbon carryover to the final particulate collector.

FABRIC FILTER INSTALLATIONS

Fabric filters have been installed on numerous fluidized-bed combustors in Europe and the United States. These fabric filters range in size from small 5.66 m^3/min (200 acfm) systems on experimental FBCs to full-scale 1130 m^3/min (40,000 acfm) units on industrial fluidized-bed boilers. Examples of fabric filters being used on FBCs in West Germany include the 35 MW_t Flingern plant in Düsseldorf and the 6 MW_t FBC located at the Köenig Ludwig Colliery in Recklinghausen. Both of these units use woven glass bags with a Teflon/graphite coating. At the Flingern plant, cleaning is accomplished by reverse air and shaking, while only reverse air is used at the Recklinghausen facility.

The results of a survey of U.S. fabric filter installations are shown in Table 2. The first full-scale fabric filter to be applied to an FBC in the United States was the Georgetown University unit which began operating in July of 1979. Other industrial-size systems include the Central Ohio Psychiatric Hospital FBC, which began operating in June of 1980, and the FBC at the Great Lakes Naval Training Center in Illinois, which is scheduled to begin operating in 1981. Georgetown is the largest of these units with a rated steam capacity of 45,400 kg/hr (100,000 lb/hr) compared to 27,240 kg/hr (60,000 lb/hr) for the Central Ohio FBC and 22,700 kg/hr (50,000 lb/hr) for the Great Lakes unit. The Georgetown and Great Lakes plants are U.S. Department of Energy (DOE) demonstration units while the Central Ohio Psychiatric Hospital facility is partially funded by the State of Ohio DOE.

The three full-scale fabric filters applied to the AFBC units discussed above reflect a range of vendor designs. The Enviro-Systems design at Georgetown employs a novel "Shock Drag" cleaning system (recently supplemented with pulse jet assist) using a combination fiberglass/nylon fabric while the American Air Filter design for Central Ohio uses off-line pulse jet cleaning with woven glass bags. Filtration velocities range from 0.46 m/min (1.5 ft/min) at Great Lakes to 1.83 m/min (6 ft/min) at Central Ohio. The design of the Great Lakes fabric filter appears to be the most conservative in that the combination of low filtration velocities and reverse air cleaning with woven glass bags closely parallels the most successful and accepted designs for fabric filters on conventional boilers.

Six pilot and experimental units using fabric filters to control particulate emissions are also listed in Table 2. The sizes of these FBC units range from EPA's Sampling and Analytical Test Rig (SATR) with a coal-burning capacity of 9.1 to 50 kg/hr (20 to 110 lb/hr), to the Electric Power Research Institute (EPRI)/Babcock-Wilcox (B&W) unit at Alliance, Ohio with a capacity of 885 kg/hr (1950 lb/hr). The fabric filter at this site uses pulse jet cleaning with felted fiberglass fabric, which is a rather recent development. The FluiDyne unit, which uses Nomex felt bags, is the only one of the six FBC fabric filters not using glass bags. Pulse jet cleaning with felt bags, either Nomex, glass

TABLE 2. FABRIC FILTERS PLANNED AND OPERATING ON ATMOSPHERIC FLUIDIZED-BED COMBUSTION UNITS—U.S.

	Georgetown University, Washington, D.C.	Central Ohio Psychiatric Hospital, Ohio	Great Lakes Naval Training Center, Ill.	Pope, Evans, and Robbins Demonstration Unit, Alexandria, Va.	Combustion Engineering Demonstration Unit, Windsor, Conn.	FluiDyne Engineering Demonstration Unit, Minneapolis, Minn.	EPRI/B&W Pilot Plant, Alliance, Ohio	SATR Experimental Unit, EPA, Research Triangle Park, N.C.	Grand Forks Energy Research Center Experimental Unit, Grand Forks, N.D.
Fabric Filter Manufacturer	Enviro-Systems & Research, Inc.	American Air Filter Co., Inc.	Zurn Industries, Inc., Air Systems Division	Buell Division, Envirotech Corporation	Combustion Engineering, Inc., Air Preheater Division	Eagle Corporation	Fuller Corporation	Young Industries, Inc.	Wheelabrator - Frye, Inc., Air Pollution Control Division
Cleaning method	Shock-Drag with pulse jet assist	Pulse jet (off-line)	Reverse air	Pulse jet and/or reverse air	Reverse air	Pulse jet	Pulse jet	Pulse jet	Pulse jet
Fabric type	Coated woven fiberglass with nylon overlay	Coated woven fiberglass	Coated woven fiberglass	Coated woven fiberglass	Coated woven fiberglass	Felted Nomex	Coated felted fiberglass	Teflon felt	Coated woven fiberglass
Design pressure	Negative, 5.04 kPa	Negative	Positive	Negative	Negative	Negative	Negative, 10.1 kPa	Positive	Negative, 1.26-2.52 kPa
Rated flue gas flow rate (m^3/min)	1275	765	675	85.0	28.3	106	230	2.8-11.3	18.4
Flue gas temperature (^oC)	180-230	205-230	175-230	205-230	150-175	180-195	190-205	175-230	120-175
Air-to-cloth ratio, gross (m/min)	1.43	1.83	0.46	-	0.46	1.14	0.79	1.83-1.98	0.70
Pressure drop (kPa)	1.01-1.51	2.02	1.51	-	1.01-1.26	0.38-0.50	0.50-0.63	1.01-1.26	<0.25
Number of bags, total	792	760	240	-	48	-	392	7	18
Number of compartments	22	4	3	-	4	1	4	1	1

or Teflon, generally permits higher filtration velocities compared to reverse air cleaned woven bags, viz., 1.52 m/min (5 ft/min) compared to 0.61 m/min (2 ft/min). Nomex is not as acid-resistant as Teflon or glass, but it is much less expensive than Teflon and possibly less subject to deterioration with repeated cleaning compared to glass fabrics.

For the small experimental systems, both FBC and fabric filter operating parameters can vary over wide ranges. Table 2 reflects the fact that pulse jet fabric filters are used more often than conventionally-designed reverse air collectors, while operating with a wide range of air-to-cloth ratios, pressure drops, and fabric types. The emphasis for many of these pilot units appears to be more on optimization of FBC parameters than on the specific design of the particulate collector. In addition, due to recognized scaling factors and the limited number of experimental measurements, pilot fabric filters are not entirely representative of expected full-scale fabric filter operation. The limitations associated with scale-up from pilot to full-scale units is also an important consideration with respect to electrostatic precipitators.

ELECTROSTATIC PRECIPITATOR INSTALLATIONS

The only operating ESP on a fluidized-bed boiler is the hot-side precipitator downstream of a four-cell AFBC at the Monongahela Power Station at Rivesville, West Virginia. Design conditions for this precipitator (designed by Buell, Division of Envirotech) include an efficiency of 99 percent on a 5750 m^3/min (203,000 acfm) gas stream at 388°C (730°F); a specific collection area (SCA) of 135 $m^2/(m^3/sec)$, (687 ft^2/1000 acfm); a 2.0 g/dsm^3 (0.87 grains/acf) inlet grain loading; and an ESP treatment velocity of 1.09 m/sec (3.57 ft/sec). Despite boiler operational instability (viz., inlet loadings and volume flow rates for the three-cell operation were higher and temperatures lower than design) precipitator performance was tested in 1979.[1] A recent 200-hour run has indicated improved ESP performance and further tests are planned to substantiate sizing criteria.[2]

A pilot ESP, designed and built by Denver Research Institute, has been installed on the SATR FBC unit at Research Triangle Park, North Carolina, although the system is not now operating. Another pilot ESP may be installed on a slipstream at the EPRI/B&W Alliance, Ohio FBC facility in order to compare the relative performance of an ESP to a fabric filter with the same fly ash and under the same boiler operating conditions.

SECTION 2

APPROACH

Five fly ash samples were obtained from four FBC sites ranging from pilot to full-scale units. As shown in Table 3, these units cover a wide range of operating conditions. Samples C and D were obtained from the same unit, without and with fly ash recycle respectively. All of the other samples except A were taken under the condition of fly ash reinjection into the boiler. In the "Results/Discussion" section, it will be shown that samples C and D contained 10.2 and 9.5 percent carbon respectively. The relatively high excess air and conservative fluidizing velocities noted in Table 3 appear to correlate well with the relatively low values for percent carbon.

Each of the four FBC sites is equipped with fabric filter collectors. Fly ash samples were extracted from the hopper at each site, screened to less than 125 μm, and riffled.[3] Aliquot test samples were then prepared for subsequent laboratory analyses, which are listed in Table 4.

All measurements of particle size distribution and filtration parameters were conducted using the GCA bench scale fabric filter test (panel) system,[4] discussed in detail in Appendix A. The fly ash samples were redispersed at high pressure into an approach duct that was connected to a fabric panel assembly. After a period of startup, a sample was extracted from a location opposite the midpoint of the panel and sized using an Andersen Mark III (eight-stage) Cascade Impactor. Replicate tests were run at a flow rate of 0.014 m^3/min (0.5 acfm) for a period of 1 to 2 minutes for sample extraction. The manufacturer's calibration data for stage jet diameters and the inertial impaction parameter were used and stage cut diameters were calculated by an iterative procedure. Cumulative particle size distributions were then plotted and the aerodynamic mass median diameter (aMMD) and the geometric standard deviation (σ_g) were obtained from a straight line fitted to the data.

The specific resistance coefficient, referred to as K_2, is simply a measure of the filterability of the dust cake on a fabric surface. Each of the FBC fly ash samples was filtered through a panel of 10 percent Teflon-B coated fiberglass fabric, which is often specified for use in fabric filter collectors applied to conventional coal-fired utility and industrial boilers. All runs were made at a filtration velocity of 0.76 m/min (2.5 ft/min) with inlet concentrations ranging from 1.60 to 2.75 g/am^3 (0.7 to 1.2 grains/acf) depending on the sample. Pressure loss across the fabric panel was monitored and the panel was periodically removed from its holder for weighing. Curves of fabric drag versus dust loading were constructed from the data collected and K_2 was determined for each ash by a linear approximation of the slope of the drag versus dust loading curve.

TABLE 3. FBC OPERATING CONDITIONS FOR FLY ASH SAMPLES*

Parameter	Facility/Sample Designation				
	EPRI/B&W Pilot Plant Alliance, Ohio	SATR Experimental Unit EPA, Research Triangle Park, North Carolina	FluiDyne Engineering Demonstration Unit Minneapolis, Minn.		Georgetown University Washington, D.C.
	A†	B‡	C†	D	E‡
Gas flow rate (m^3/min)	230	2.8-11.3	59.4	60.8	1275
Bed temperature (°C)	840	790-855	840	830	870
Coal feed rate (kg/hr)	885	9-50	233	234	4345
Calcium-to-sulfur ratio, Ca/S (mole/mole)	3.4	3.0	2.8	2.3	3.0§
Excess air (%)	18	25	33	32	20
Fluidizing velocity (m/sec)	2.4	0.91-4.9	1.3	1.3	2.4
Air-to-cloth ratio, A/C (m/min)	0.61	1.98 max.	0.64	0.67	1.34

*Fly ash samples were extracted from the fabric filter hopper at each site.

†Sample taken without fly ash reinjection.

‡Design conditions.

§Ca/S during sample extraction was 4 to 5.

TABLE 4. SUMMARY OF FBC FLY ASH MEASUREMENTS

Parameter/analysis	Instrument/technique
Particle size distribution	Andersen Mark III (eight-stage) cascade impactor
Specific resistance coefficient	GCA/Technology Division bench scale fabric filter test panel system
Resistivity	Denver Research Institute single and multiple cell resistivity apparatus
Chemical/spectral analysis	Amray Model 1200 SEM* with EDXRA†
Carbon analysis	Low temperature ashing (LOI)‡ High temperature ashing (CHN)§
Morphology	Amray Model 1200 SEM*

*Scanning Electron Microscope

†Energy Dispersive X-ray Analysis unit

‡Loss on Ignition

§Carbon-Hydrogen-Nitrogen test using a Perkin Elmer Model 240B Elemental Analyzer

Resistivity measurements for the fly ash samples were conducted by Denver Research Institute using a parallel plate resistivity cell apparatus,[5] discussed in detail in Appendix B. Electrical resistivity was determined by measuring the current conducted through the sample under an applied voltage of approximately 3940 volts/cm (10,000 volts/inch). The resistivity cell is housed in an electrically controlled oven to allow variation in temperature from 120 to 400°C (250 to 750°F). Humidity was set at 5, 10, and 20 percent H_2O by volume, by passing the air through one of three temperature-controlled fritted glass water bubblers.

Chemical analysis of the fly ash samples was accomplished by using a scanning electron microscope (SEM), also used for particle morphology analysis, integrated with an energy dispersive X-ray analysis unit (EDXRA). This system, discussed in detail in Appendix C, provides approximate quantitative elemental analyses of individual particles or a field of particles. Although not an absolute indicator of all chemical elements present (it is limited, for example, by the small sample size used which may not be representative of the total sample), elements attributed to the following oxides were measured: aluminum (Al_2O_3), silicon (SiO_2), calcium (CaO), iron (Fe_2O_3), potassium (K_2O), and titanium (TiO_2).

As part of an effort to correlate electrical and chemical properties of the five FBC fly ash samples, two techniques were employed to assess the free carbon concentration present in the samples. Initially, a simple loss on ignition (LOI) analysis was performed whereby desiccated weights of each sample were taken before and after being placed in a flow ashing chamber. This procedure was repeated after the samples had been treated with hydrochloric acid to remove any carbonates present. These steps were supplemented with a carbon-hydrogen-nitrogen (CHN) test. This procedure involves the high temperature ashing of a fly ash sample in the presence of a reagent to provide excess O_2 for complete combustion. The off-gases are passed through a gas chromatograph column to separate and identify the oxides present.

FABRIC FILTER MODEL

Under contract with the U.S. Environmental Protection Agency, GCA/Technology Division has developed a working mathematical model that can be used to predict the field performance of large fabric filter systems applied to coal-fired utility boilers.[4,6,7] The model applies to specific collector types using woven glass fabrics with any of several surface treatments and simulates fabric cleaning by a collapse and reverse flow process and/or shake assist. The model takes into account the physical properties of the boiler effluent, the basic design and operating parameters of the filter collector as well as the filtration parameters associated with the dust and fabric. Both average and instantaneous pressure drop and particle penetration as a function of time can be predicted. Comparison of the model results with measured field data on fabric filters applied to conventional boilers at the Sunbury Station of Pennsylvania Power and Light and the Nucla Station of Colorado-Ute Electric Association, has shown excellent agreement with respect to filter system performance.

Several key concepts, based largely on laboratory and pilot testing, form the basis for the model simulation of full-scale fabric filter operation and performance. The model simulates the distribution of gas flow to a number of parallel compartments of the collector. Resistance to flow created by the dust cake is a function of the velocity at which the dust is deposited on the fabric and the thickness of the deposit. Removal of dust from a bag is nonuniform in that some portions of the fabric surface retain a complete dust layer after cleaning whereas others shed all of the deposited dust, except for a small residual amount which remains embedded in the fabric. With respect to dust penetration, the model reflects the results of test observations which conclude that no appreciable particle size segregation occurs. Finally, the penetration of dust through the dust/fabric medium is a function of the dust cake thickness as well as the filtration velocity.

The following fabric filter design parameters are required as input to the model: number of compartments, cleaning method, cleaning schedule, and reverse flow velocity. Required operating parameters include flue gas temperature, inlet dust concentration, and gross filtration velocity (air-to-cloth ratio). Important inlet dust properties to be considered include the specific resistance of the dust cake, K_2, and the effective residual drag of the fabric and dust combination, S_E. These two parameters define a straight line on a fabric drag versus loading plot that relates the overall resistance to flow created by the fabric and the dust, to the amount of dust on the fabric. Finally, an estimate of the degree of cleaning that can be expected must be made. This parameter, referred to as a_c, relates the amount of dust removed from a bag to the amount of dust present before it is cleaned.

In this study the effects of K_2 on penetration and pressure drop across the fabric as a function of the filter face velocity and a_c are examined.[8] In order to conceptually examine the relationships among key performance and design parameters, an "average system" is defined with respect to the parameters discussed above.

ELECTROSTATIC PRECIPITATOR MODEL

In recent years, increasing attention has been given to the development of theoretical relationships that describe the physical, chemical, and electrostatic mechanisms interacting in the electrostatic precipitation process. Under EPA sponsorship, Southern Research Institute (SoRI) has developed a mathematical computer model that incorporates many of these relationships.[9,10] The model depends on the basic Deutsch-Anderson equation to calculate the particle collection efficiency for each incremental length along the precipitator collecting plate. A key parameter in this relation is the particle migration velocity (or particle drift velocity) which is a function of electrical energization of the precipitator, gas properties, and entering particle size distribution. In the model, migration velocity is calculated using field and diffusion charging theories, and is adjusted using empirical correction factors to account for unmodeled effects. The model also accounts for the nonideal effects of nonuniform gas velocity distribution, gas bypassage of electrified regions, and particle reentrainment due to rapping and other causes. Overall collection efficiency is estimated by summing the incremental collection

efficiencies over the entire precipitator length and iteration is exercised until a convergence on the overall collection efficiency is obtained. Estimation of nonideal collection efficiencies is accomplished by adjusting the ideal efficiencies for nonideal effects after convergence is obtained.

The model can be used as a tool in troubleshooting precipitators that are not meeting the overall mass collection efficiency that is expected or anticipated. To exercise this feature, certain experimental data are required, such as operating voltages and currents, inlet mass loading and particle size distribution, ash resistivity, average gas flow rate and velocity, and average temperature and pressure. Furthermore, with proper care in selection of input data, the model can be used as a rough guide in precipitator design.

The SoRI/EPA model was used in this study to investigate the relationship between specific collection area (SCA) and overall mass collection efficiency using measured resistivity and particle size distribution data for three FBC fly ash samples. (Samples A and E were not considered due to abnormally low resistivities as discussed in the next section.) Assumptions regarding other factors such as flue gas properties and current-voltage characteristics were made on the basis of past experience in using the model as well as on model validation tests conducted by SoRI. The model is also used to demonstrate the effect of particle size distribution on efficiency.

SECTION 3

RESULTS/DISCUSSION

Table 5 shows the results of resistivity, particle chemical composition, particle size distribution, and filtration measurements conducted on each of the five FBC fly ash samples. These results are used in conjunction with other assumptions to examine the relationships among key design and performance parameters for fabric filters and ESPs used in FBC applications.

With respect to electrical resistivity, samples B, C and D exhibit values that fall within the moderate to high range generally observed with conventional coal-fired boiler fly ash. The characteristic variation of resistivity with temperature is also observed. The fact that samples A and E have such unusually low resistivities is attributed to the rather high carbon contents present, as determined by both simple LOI and CHN analyses. In fact, due to these high carbon contents, samples A and E exhibited spark over at 260°C (500°F) and, as a result, further measurements could not be made.

As discussed earlier, two methods were used to determine the amount of carbon (combustibles) present in each sample. While the weight loss of a sample associated with simple LOI analysis is usually representative of carbon content, losses from other carbonaceous matter such as carbonates and volatile species, if they are present, will be reflected in the results. In order to determine the carbonate contribution to the LOI results, the LOI analysis was repeated after the sample had been treated with hydrochloric acid to remove any carbonates. These results are, within experimental error, identical to those from the simple LOI test. It may be inferred, therefore, that the carbonate content of the samples is relatively small. A CHN analysis yielded results that are in good agreement with the LOI results (see Table 5). In the absence of carbonates, the CHN data provide an excellent characterization of the free carbon constituent.

The chemical analysis presented in Table 5 is not intended to be a comprehensive assessment of all of the oxides present. Spectral analysis using an SEM in conjunction with EDXRA is limited by the small sample size used in the apparatus (which may not be representative of the whole sample) as well as by the fact that even with computer correction, some elements are more responsive to X-ray analysis than others. Silicon, for example, is more efficiently excited by X-rays whereas sulfur, below 4 percent by weight, is usually not detectable.

TABLE 5. RESULTS OF FUNDAMENTAL MEASUREMENTS PERFORMED ON FBC FLY ASH SAMPLES

Sample designation	Resistivity (ohm-cm) @ 10% moisture			Chemical/spectral analysis* constituents (% by weight)							Particle size distribution		Specific surface parameter, S_o^2 (x $10^{-\theta}$)†	Specific resistance coefficient, K_2
	149°C	260°C	370°C	Al_2O_3	SiO_2	K_2O	CaO	TiO_2	Fe_2O_3	C‡	aMMD, $\overline{x}$ (μm)	σ_g	(cm^{-2})	(N-min/g-m)
A§ - Alliance	3.3×10^7	1.2×10^7	#	11.1	33.2	1.8	10.1	1.0	4.1	33.7	6.0	2.8	5.77	4.89
B - SATR	3.2×10^{11}	5.0×10^{10}	5.0×10^9	21.4	48.5	1.7	10.7	1.6	3.6	7.5	5.3	2.6	6.39	5.25
C§ - FluiDyne	8.0×10^{11}	1.4×10^{11}	5.0×10^9	12.0	39.5	3.0	20.7	1.8	7.8	10.2	7.3	2.6	3.37	1.94
D - FluiDyne	1.1×10^{12}	2.6×10^{11}	8.0×10^9	12.3	40.0	3.0	22.6	1.0	7.6	9.5	8.9	3.0	3.04	2.46
E - Georgetown	7.1×10^5	3.3×10^5	#	9.9	24.2	1.3	7.0	-	6.4	46.2	7.7	2.7	3.26	4.74

*The six oxides were derived from SEM/EDXR analysis. This method is relatively insensitive to elements of low atomic number. Some elements (attributed to their common oxides, e.g., SO_3) could not be measured, hence the total does not equal 100%.

†The specific surface parameter, S_o^2, can be calculated from the particle size distribution parameters by the formula

$$S_o^2 = \left[6\left(\frac{10^{1.151 \log^2 \sigma_g}}{MMD}\right)\right]^2$$

. Particle density, used to convert aMMD to MMD, was assumed to be 2.0 g/cm^3.

‡Percent carbon was determined using a CHN test. Results closely agree with those from a simple LOI determination. For samples A, B, C, D, and E, the percent combustibles (LOIs) were 25.9, 7.5, 12.4, 10.9, and 43.0, respectively.

§Without fly ash reinjection.

#Both samples A and E sparked over above 260°C (500°F), hence, testing could not be continued.

Table 5 also shows that the specific resistance coefficient, K_2, of the FBC fly ash samples varies from 1.94 to 5.25 N-min/g-m (11.6 to 31.4 in. W.C.-min-ft/lb). Filtration theory predicts that K_2 increases with decreasing particle size. A specific surface parameter, S_o^2, calculated from the mass median diameter and geometric standard deviation of a dust sample, may be used to characterize this relationship between K_2 and particle size.[4] The computed values of S_o^2 in Table 5 appear to be correlated with measured K_2 (correlation coefficient r = 0.73). The actual point scatter may be attributed to differences in particle shape, surface characteristics, or charge effects, although additional investigation is needed to resolve this issue.

Figures 1 and 2 provide a comparison of FBC fly ash morphology with conventional coal-fired fly ash particle morphology. These photomicrographs illustrate the fact that conventional fly ash is generally more spherical in nature whereas FBC fly ash represents a broad composition of irregularly-shaped particles. Particle surface characteristics can be important in dust cake buildup and in dust cake porosity for fabric filters. Surface characteristics can also be important in how fly ash is naturally conditioned within the gas stream so as to enhance electrostatic precipitation. Clearly more work has to be done to substantiate how fly ash morphology affects collection by filtration and electrostatic precipitation.

FABRIC FILTER ANALYSIS

Filterability of the dust cake is an important parameter in predicting filter penetration and pressure drop. As noted in Table 5, the filterability parameter (K_2) varies by a factor of 2.5 over the five FBC fly ash samples tested. In order to examine this variation in K_2, the GCA fabric filter mathematical model described earlier was used. For this conceptual analysis, an average fabric filter system was defined, consisting of 14 compartments, a 35-minute cleaning cycle, and a reverse flow velocity of 0.61 m/min (2 ft/min). To simulate AFBC boiler effluent, an uncontrolled particulate concentration of 8.0 g/dsm^3 (3.5 grains/acf) and a gas temperature of 205°C (400°F) were chosen. The value of K_2 was chosen to be 5.0 N-min/g-m (30 in. W.C.-min-ft/lb) in contrast to 2.0 N-min/g-m (12 in. W.C.-min-ft/lb), a value which is reported for conventional coal-fired boiler fly ash.[4] With respect to the woven glass fabric and dust combination, a representative value of 400 N-min/m^3 (0.49 in. W.C.-min/ft) was selected for S_E.[4]

Under the assumption that FBC fly ash is removed from the fabric surface during cleaning to the same degree as conventional fly ash, Figures 3 and 4 show the effect of K_2 on penetration and pressure drop respectively as a function of filter face velocity. The higher K_2 associated with FBC fly ash results in a higher pressure drop and higher local velocities through "relatively clean" fabric areas, which cause increased particle "seep-through" (penetration) compared to the conventional fly ash case. At an air-to-cloth ratio of 0.61 m/min (2 ft/min), the difference in K_2 results in roughly a 30 percent increase in fractional penetration and a 100 percent increase in pressure drop. To achieve a collection efficiency of 99.5 percent, for example, a 0.91 m/min (3 ft/min) filtering velocity would be acceptable with

Figure 1. Representative morphology for FBC fly ash.

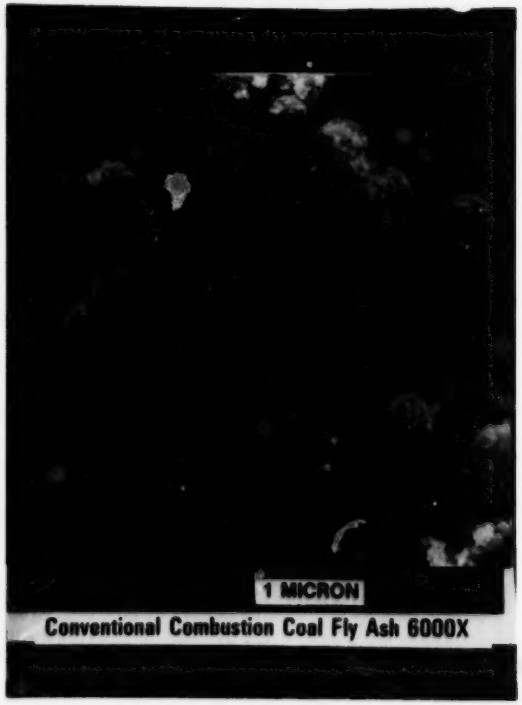

Figure 2. Representative morphology for conventional coal-fired boiler fly ash.

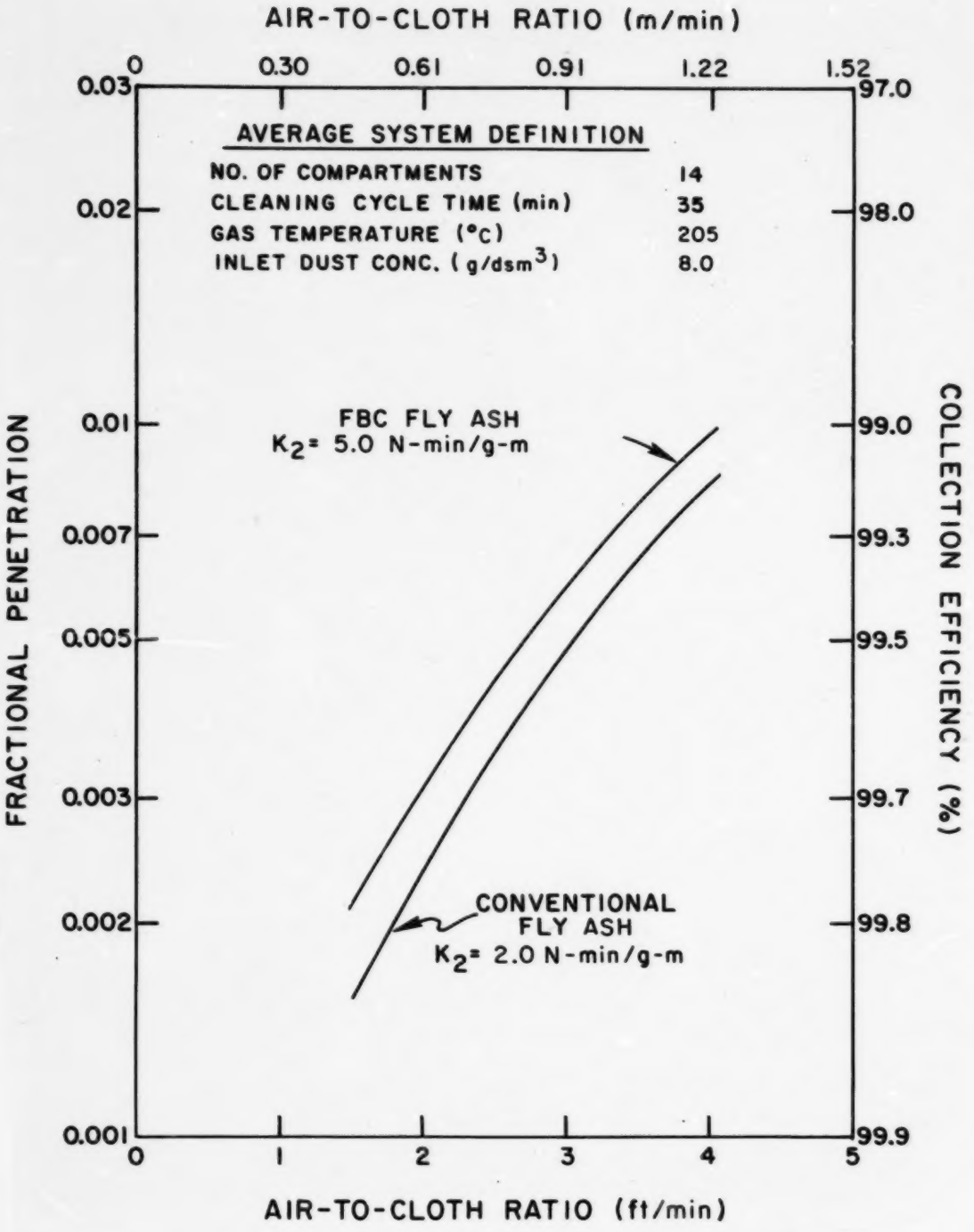

Figure 3. The effect of air-to-cloth ratio on particle penetration for different K_2 levels.

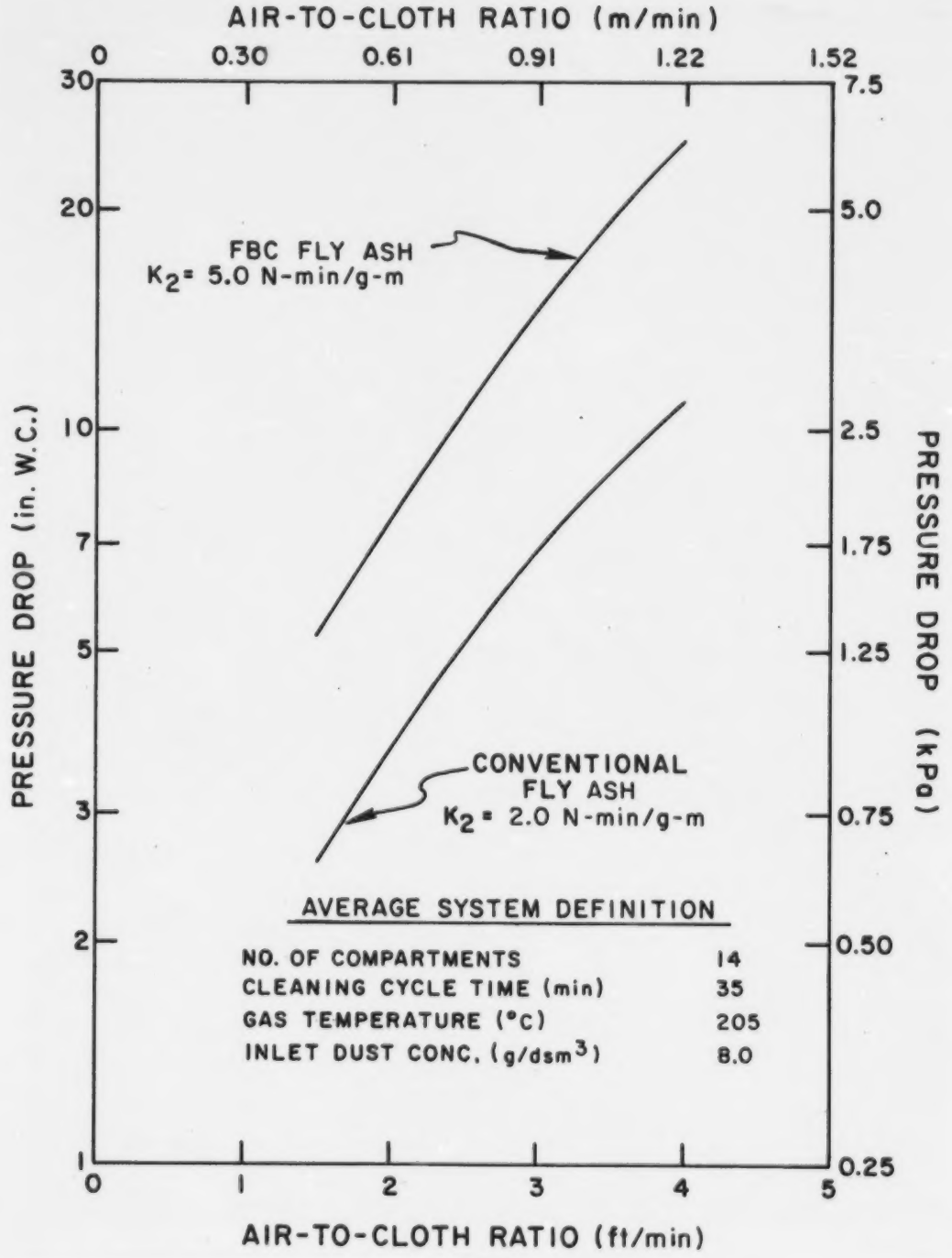

Figure 4. The effect of air-to-cloth ratio on filter pressure drop for different K_2 levels.

a fly ash having the lower K_2, but not with a fly ash at the higher K_2 level. Although these are modeled results, they do describe conceptually the effect of a less porous dust cake (high K_2), the resultant higher pressure drop, and that particle seep-through under the driving force of higher local velocities can account for increased filter penetration.

If it is found that FBC fly ash does not have dust-fabric release properties similar to conventional fly ash, then the "cleanability" of the fabric would be expected to be different. The cleanability parameter, more properly termed the fraction of the filter area cleaned, is simply an indicator of how much dust is removed from a woven glass bag during reverse air or shake cleaning. The degree of cleaning is determined by model calculation based on experience with conventional fly ash. For a K_2 of 5.0 N-min/g-m (30 in. W.C.-min-ft/lb) and an air-to-cloth ratio of 0.61 m/min (2 ft/min), the model calculates that approximately 25 percent of the fly ash is removed upon cleaning. Figure 5 shows how penetration and pressure drop will vary as a function of the degree of cleaning. If less than 25 percent of the filter cake is removed, pressure drop increases considerably with only a slight decrease in penetration. (This is due to the fact that more of the filter cake is present to filter additional fly ash.) With a greater degree of cleaning compared to conventional fly ash, more of the dust cake is removed, the pressure drop decreases but the penetration increases. As the degree of cleaning increases from 10 to 40 percent, pressure drop is reduced by approximately 70 percent while penetration increases by roughly 12 percent. Clearly, the ease of dust removal from the bag surface as a result of cleaning is an important factor in predicting fabric filter operating pressure drop and performance.

ELECTROSTATIC PRECIPITATOR ANALYSIS

Particle resistivity is an important consideration in the application of electrostatic precipitators to fluidized-bed combustion. Very low concentrations of SO_3 have been recorded in FBC flue gas, which implies a reduced conditioning effect on the particles, resulting in increased resistivity. In addition, all sorbent materials ($CaCO_3$, CaO, MgO, and $CaSO_4$) have high resistivities. However, carbon content exerts a strong influence in lowering fly ash resistivity.

Resistivity measurements for each of the five fly ash samples studied are compared with other reported data as shown in Figure 6. The resistivity curves for samples B, C, and D at 10 percent moisture, closely resemble one another and attain their maximum resistivities at 149 to 177°C (300 to 350°F). The characteristic shape of these curves and the magnitude of the measurements are in agreement with measurements obtained by Pope, Evans, and Robbins for fly ash samples from their Alexandria FBC facility.[11]

The resistivities of samples A and E are similar to one of the test runs conducted on fly ash from the Rivesville hot-side ESP. The carbon content of the Rivesville sample was found to be 47 percent, which compares to the relatively high percent combustibles noted for samples A and E (see Table 5). While the Rivesville FBC has four cells (three main cells and one carbon burnup cell), only one cell was operating when the test was run. Examination

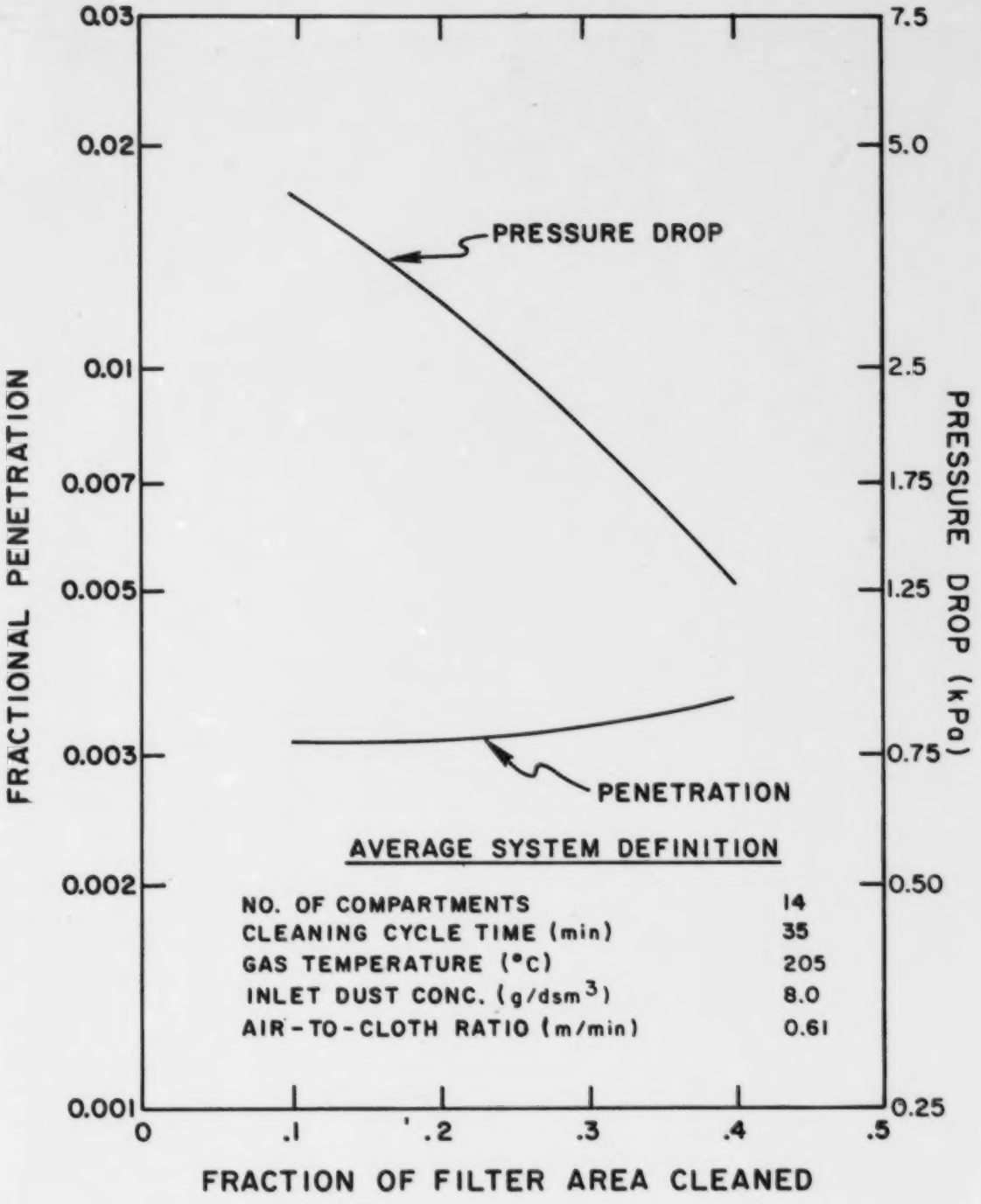

Figure 5. Penetration and filter pressure drop as a function of fraction of filter area cleaned (K_2 = 5.0 N-min/g-m).

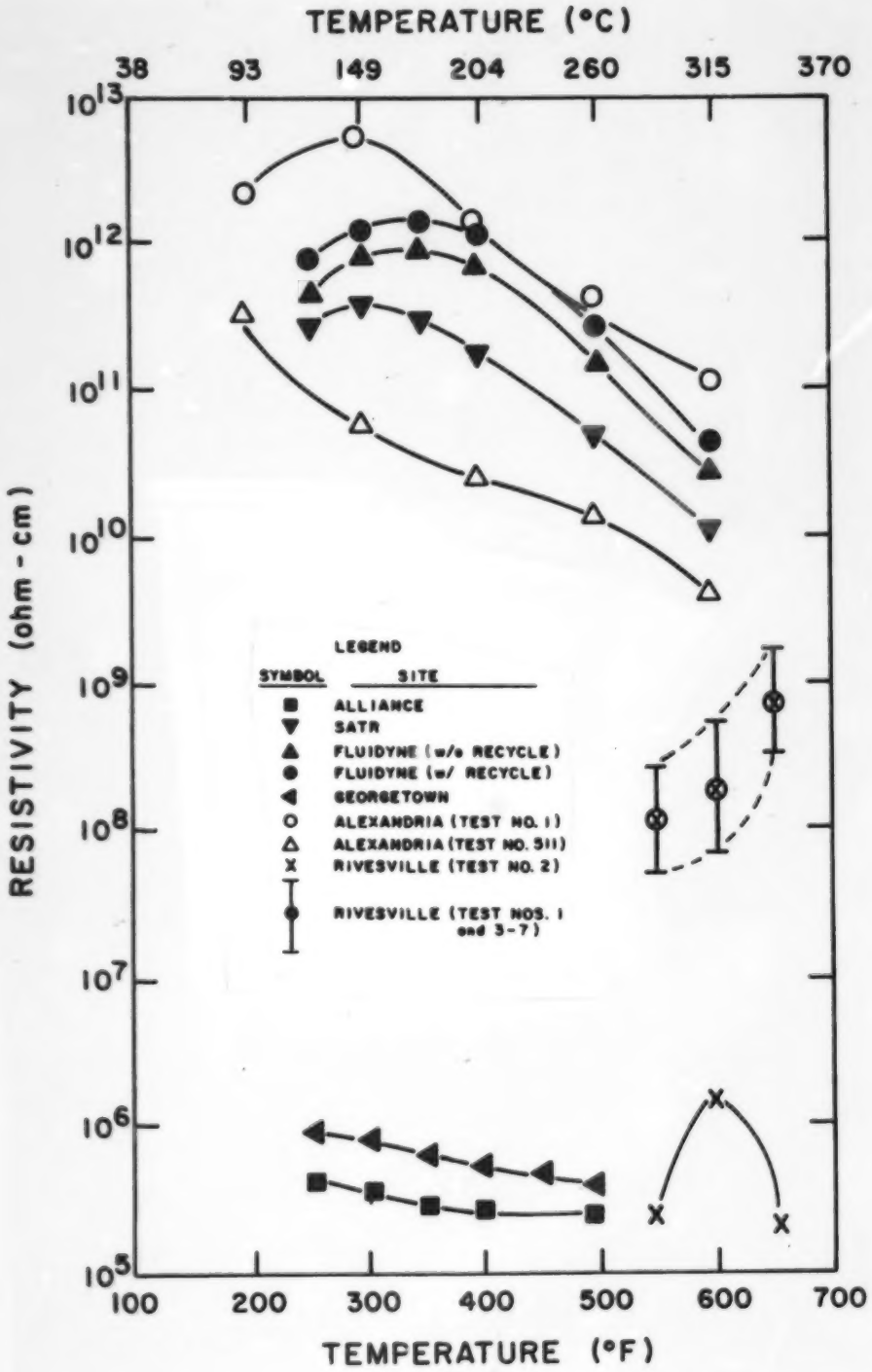

Figure 6. Summary of resistivity data.

of Alliance and Georgetown operating data revealed that sample E was obtained at low load conditions while sample A was obtained without fly ash recycle. Based on these observations, the high carbon contents of these samples can be attributed to the low collection efficiency of the precollectors or cyclones under low load conditions and, in one case, the lack of recycle. Also shown in Figure 6 is a band of other resistivity measurements (ranging from 10^8 to 10^9 ohm-cm) for Rivesville fly ash. These samples were obtained when the carbon burnup cell was not operating and contained 20 to 25 percent carbon.[11]

For conventionally generated fly ash, carbon contents above 8 to 10 percent have been found to be an important factor in decreasing resistivity.[12] The results shown in Figure 6 suggest that resistivity of FBC fly ash is substantially reduced when the carbon content is above 20 percent by weight. In view of the conditions that promote high carbon carryover in an AFBC unit, it may be a more significant operating problem than in conventional combustion. This emphasizes the importance of the primary cyclone in providing reliable, high efficiency particulate collection capability so that unburned carbon is returned to the boiler for efficient combustion and the downstream collector is protected from the effects of carbon carryover.

Figure 7 shows the effect of fly ash resistivity on cold ESP overall mass collection efficiency as a function of specific collection area. The slope of the reference line reflects the exponential design relationship between SCA and collection efficiency. The two points shown correspond to actual design cases for conventional combustion of a high sodium lignite coal (10^9 ohm-cm resistivity) and a low sulfur western U.S. bituminous coal (10^{13} ohm-cm resistivity). The SoRI electrostatic precipitator model was used to predict the collection efficiencies at an SCA of approximately 49.3 $m^2/(m^3/sec)$, (250 $ft^2/1000$ acfm) for samples B, C, and D using their measured resistivities at 149°C (300°F) and particle size distributions. These results were extrapolated over a range of SCAs using the slope of the reference line as shown by the cross-hatched band. It is noted that the predicted SCA requirements for samples B, C, and D with resistivities between 10^{11} and 10^{12} ohm-cm, fall within the range of design experience for cold ESPs applied to the collection of conventional fly ash. Under the assumptions used to generate the band for cold ESPs, the hot ESP band would be expected to lie parallel to and above the existing cross-hatched area.

The SoRI model was also used to investigate particle size effects on ESP performance. Figure 8 summarizes the particle size distributions obtained for five FBC fly ash samples compared to pulverized coal combustion fly ash.[13] Since the FBC samples were obtained from a fabric filter preceded by cyclones, their finer size relative to conventional fly ash is attributed to the capability of the cyclones to collect coarse particles. With the exception of samples A and C, the finer particle sizes for FBC fly ash may also result, in part, from attrition when primary cyclone materials are reinjected into the boiler.

Figure 9 shows the effect of particle size distribution on the performance of ESPs. The lower broken line represents the predicted performance at 149°C (300°F) for sample B whose aerodynamic mass median diameter and geometric standard deviation are 5.3 μm and 2.6 respectively. The upper broken line corresponds

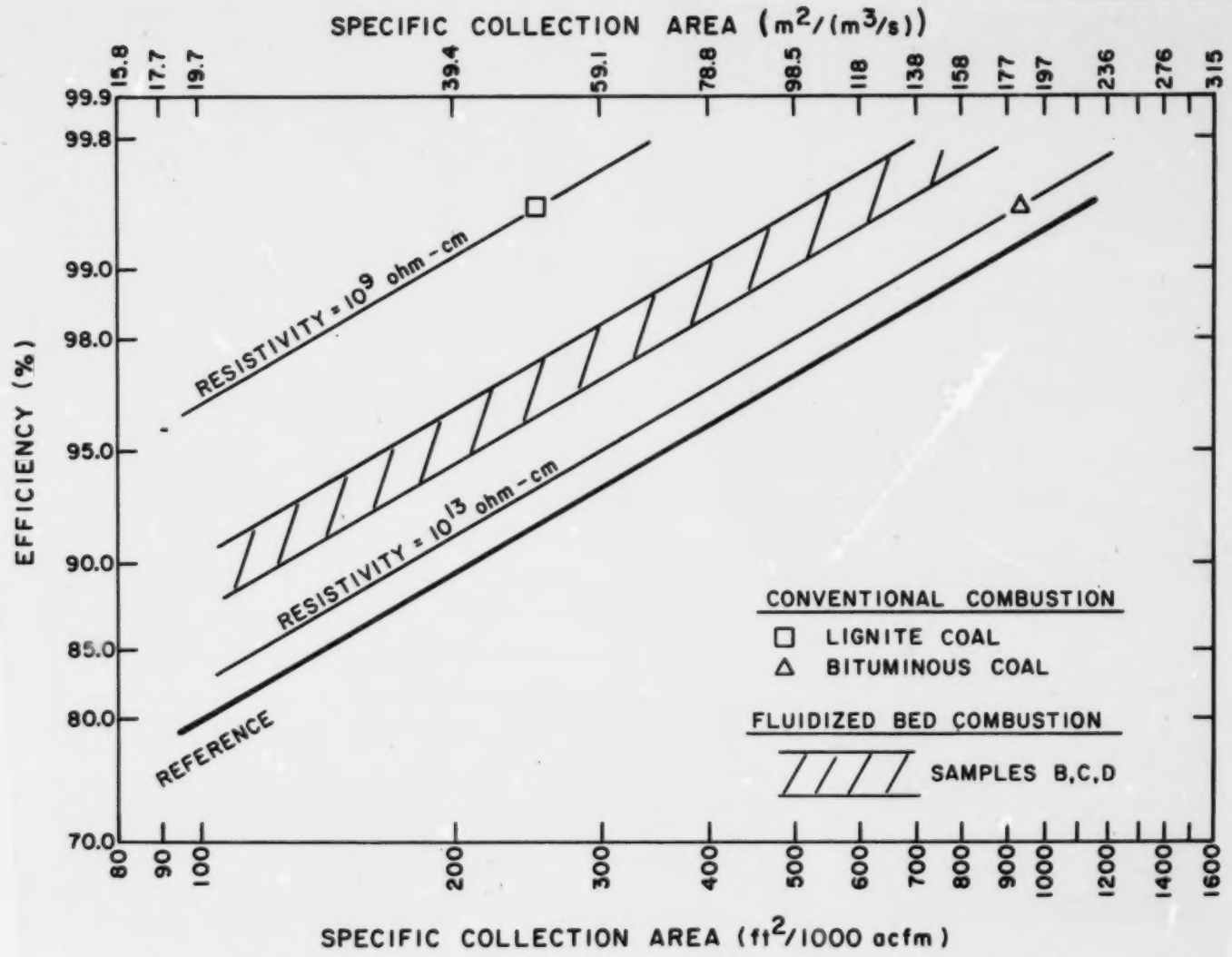

Figure 7. Effect of fly ash resistivity on cold ESP overall mass collection efficiency as a function of specific collection area.

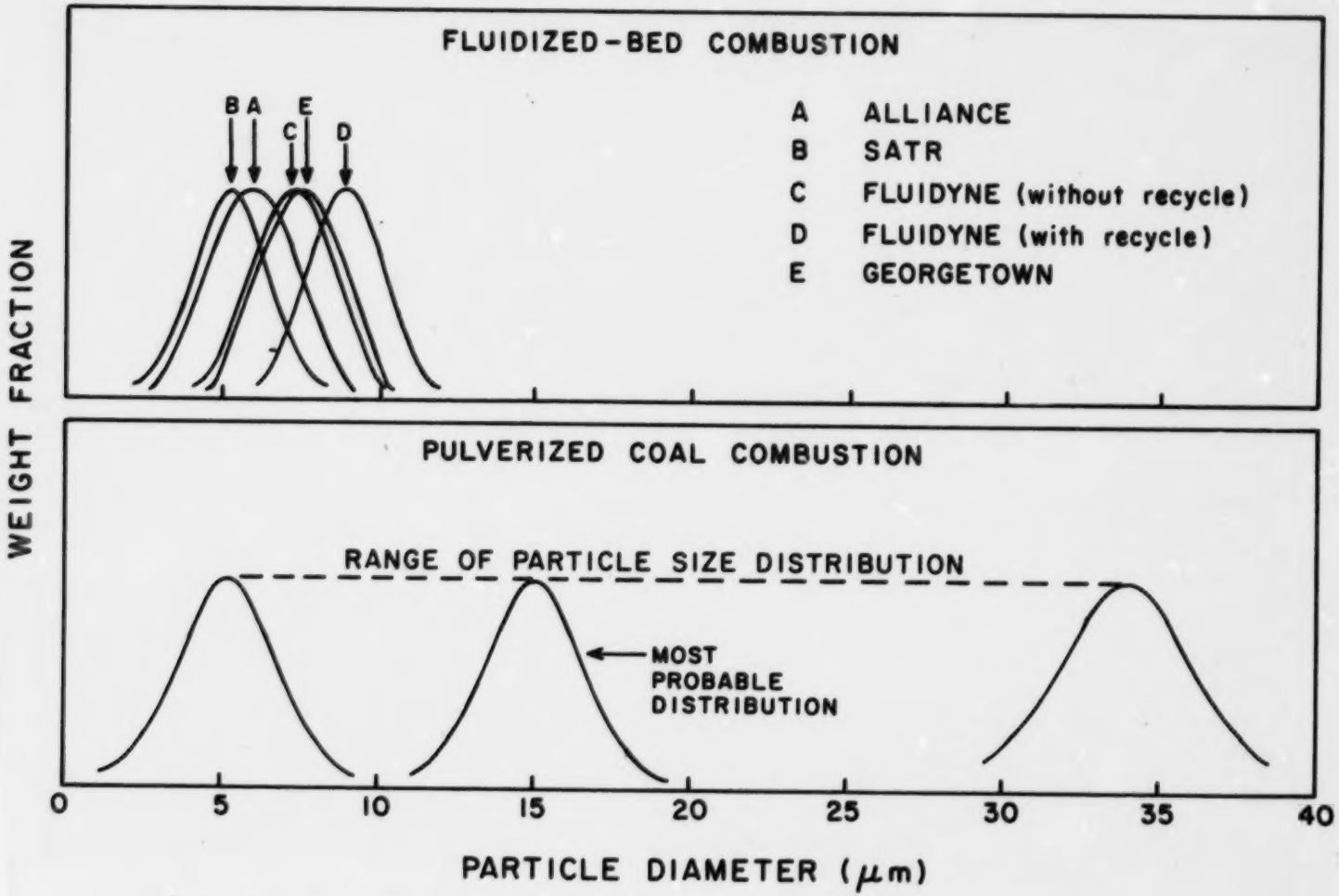

Figure 8. Summary of fly ash particle size distributions. (The spread of each distribution is not drawn to scale.)

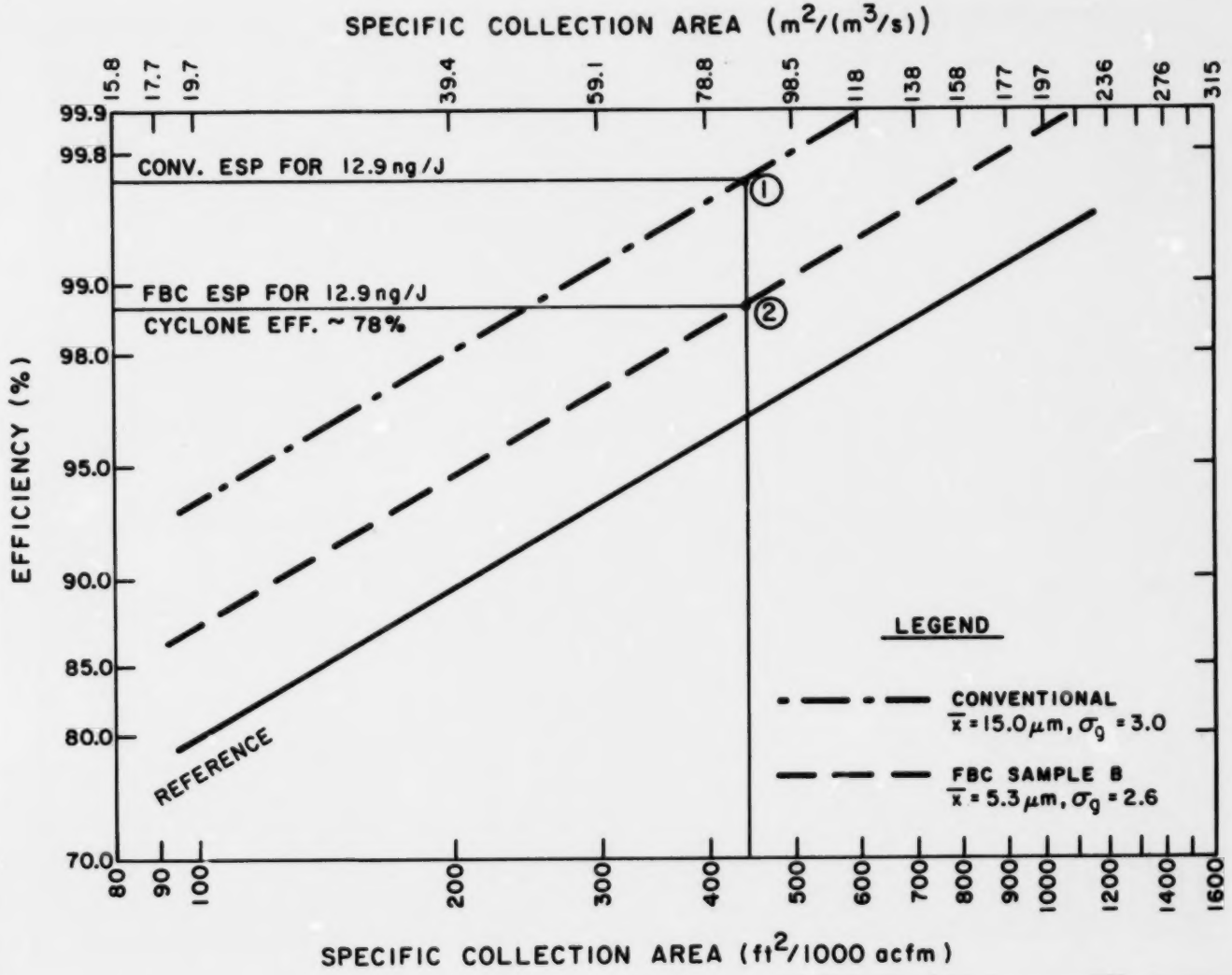

Figure 9. Effect of particle size distribution on cold ESP overall mass collection efficiency as a function of specific collection area.

to a conventional fly ash with the same resistivity as sample B. The mass median diameter and geometric standard deviation were assumed to be 15.0 μm and 3.0 respectively. It is evident from these results that the collection of smaller particles requires a larger precipitator for a given efficiency, provided that all other factors are held constant. In comparing an FBC system to a conventional combustion system generating the same amount of fly ash from the boiler, the collection efficiency of the cyclones in the FBC system must be considered. For example, point "1" on Figure 9 represents the ESP efficiency and SCA requirements for a conventional system without cyclones to meet a particulate emissions standard of 12.9 ng/J (0.03 lb/10^6 Btu). Point "2" illustrates the fact that if the cyclones in the FBC system have a combined efficiency of 78 percent or more, then a comparable or smaller SCA will be capable of achieving the same overall mass emissions standard. Thus, the fact that FBC fly ash is generally smaller than conventional fly ash (see also Figures 1 and 2) does not necessarily imply a higher SCA requirement. Depending on the collection efficiencies of the cyclones, as well as other important factors such as rapping reentrainment losses, however, a more conservative estimate of SCA may be required.

FIELD OPERATING CONSIDERATIONS

Some of the more common problem areas encountered with fabric filter operation include fabric/dust deposit interaction, bag failures, design or maintenance failures relating to bag support and the cleaning mechanism, and structural design problems including isolation dampers and the ash removal system. One of the most important areas for maintenance has to do with interactions between the fabric and the dust.[14] This includes the manner in which the dust deposits on the fabric, the ease with which it is removed, and any damage to the fabric caused by the dust. Choice of the wrong fabric can result in excessive penetration due to the development of pinhole leaks and inadequate bag service life. A dust which is hygroscopic may, in the presence of moisture, cause blinding, impede proper cleaning, cause excessive pressure buildup across the fabric, reduce bag service life, and promote ash removal problems.

With regard to fabric filters applied to FBC boilers, the presence of any appreciable amounts of calcium compounds in the fly ash would suggest that increased attention be given to the use of hopper heaters and insulation to prevent moisture accumulation and subsequent fly ash bridging in the hoppers. This would also be an important consideration for electrostatic precipitators applied to FBC. In addition, the concern for possible bag plugging would suggest the use of continuous warm air flow during maintenance and shutdown periods to prevent moisture accumulation on the bags.

The carryover of unburned carbon during startup or during a transient boiler condition may cause fabric blinding and permanent damage. For this reason it may be advisable to consider introducing fly ash ahead of the fabric filter to coat the bags and thereby protect them from atypical FBC operating conditions. At one coal-fired conventional utility fabric filter installation, dolomite lime was used to precoat the bags.[15] It was suspected that when the baghouse was shut down and opened for inspection, the residual dolomite coating on the bag absorbed moisture, resulting in higher pressure drop across the

bags compared to the case when a fly ash precoat was used. Moreover, since atypical FBC operation may sometimes entail the carryover of unreacted limestone (as well as unburned carbon), a fly ash precoat would be the optimum choice to protect the bags and keep pressure drop to a minimum.

Potential problem area considerations for precipitators applied to FBC units will include: electrode fouling due to buildup of fly ash on the wires; incidence of local burning on the wires due to high carbon carryover (and manifested by heavy sparking); rapping reentrainment losses; and transient conditions associated with boiler startup.[2]

One of the most important factors that will affect both mass and fractional collection efficiency capabilities of an ESP is rapping reentrainment losses. Under a research program sponsored by the Electric Power Research Institute ivestigating rapping reentrainment emissions from six full-scale ESPs servicing conventional coal-fired boilers, it was found that a significant portion of the total mass emissions was caused by reentrainment of coarse particles. For the hot-side ESPs tested, 60 to 85 percent of the total mass emissions was attributed to rapping, whereas only 30 percent was noted for cold-side units.[16,17,18] The high rapping losses were thought to be caused by reduced dust cohesivity at high temperatures and/or relatively short rapping intervals (as noted at one of the hot-side installations tested). Since rapping losses constitute a major fraction of the overall penetration, optimization of the ESP cleaning system, whether for FBC or conventional boilers, will be an important factor in reducing emissions.

SECTION 4

SUMMARY/FUTURE WORK

Fabric filters are being installed on many new AFBC units despite the lack of comprehensive test or demonstration data. This appears to stem in part from their increasing use on industrial and utility conventional boilers to meet more stringent mass collection efficiency and opacity requirements. An analysis of fundamental filtration parameters using redispersed fly ash in a filter test panel assembly has shown that filtration of certain FBC fly ashes may be more difficult than conventional fly ash. In three out of five FBC fly ash samples tested, the filterability parameter (or specific resistance coefficient) was noted to exceed twice that normally observed for conventional fly ash. Particle size distribution may account for the noted differences in filterability. It is suspected that charge effects or particle shape factors may also be responsible. Fabric cleanability is also an important consideration since pressure drop across the fabric increases significantly when only a small fraction of the dust is effectively removed from the bag surface.

Electrostatic precipitators have a limited operating history on AFBC units. Early difficulties at the Rivesville hot-side ESP were attributed to unstable boiler operation. A recent 200-hour run has indicated improved collector performance and further tests are planned to substantiate sizing criteria.

Comparison of measured resistivities of the five fly ash samples investigated in this study with other reported data shows a strong correlation between percent combustibles and resistivity. Combustibles contents, consisting mainly of free carbon, in excess of 20 percent by weight can reduce resistivities; in some cases to levels below optimum (viz., below 2.0×10^{10} ohm-cm). Other measurements confirm the suspected effect of low SO_3 on the FBC fly ash in that resistivities fall within the moderate to high range of design experience with ESPs applied to conventional coal-fired utility and industrial boilers. The observed finer particle size distribution of FBC fly ash compared to conventional fly ash does not necessarily imply a higher SCA requirement, although depending on the collection efficiency of the cyclone as well as other important factors such as rapping reentrainment losses, a more conservative SCA may be required.

It is clear that the performance of the final particulate collector depends on the FBC operating parameters, and in particular on cyclone efficiency, carbon burnup cell combustion efficiency, optimized freeboard height, bed depth, and fluidizing velocity. Carbon carryover, for example, can cause

severe deterioration of electrical conditions in an ESP, with the possibility of ignition and fire. This latter problem is also of concern with fabric filters, as well as the possibility of fabric blinding. Low load conditions can reduce cyclone efficiency and add to the carbon carryover problem. One important conclusion of this report is that the precollector or cyclone must be considered as an integral part of the total particulate control system. Furthermore, the entire collector system must be flexible enough in both design and operation to handle most of the potential transient conditions in AFBC operation.

With regard to future plans, under EPA sponsorship GCA will be conducting a comprehensive evaluation of the Georgetown University fabric filter in early 1981. The primary objectives will be to determine total mass and fractional particle size collection efficiencies at full and partial loads. To accomplish these goals, a 4-week field program emphasizing simultaneous particulate measurements before and after the fabric filter will be conducted. Total particulate mass concentration for particle sizes in the range of 0.5 to 15 μm will be determined using EPA Method 5 and cascade impactors. This will be supplemented with particle number concentration measurements in the size range of 0.03 to 10 μm using diffusion batteries, condensation nuclei counters, and electro-optical particle counters. EPA may sponsor similar tests at other large-scale facilities using fabric filters or electrostatic precipitators as these units come on-line.

REFERENCES

1. Buell Emissions Control Division, Envirotech Corporation. Precipitation Performance Evaluation at Monongahela Power Company, Rivesville Unit #3, Rivesville, West Virginia. Prepared for Pope, Evans, and Robbins. September 1979.

2. Shilling, N. Z., and W. J. Morris. The Response of Hot-Side Electrostatic Precipitators and Fabric Filters to Fluidized-Bed Combustors. In: Proceedings of the 6th International Conference on Fluidized-Bed Combustion, Atlanta, Georgia. April 9-11, 1980.

3. American Society for Testing and Materials. Standard Method of Preparing Coal Samples for Analysis. ANSI/ASTM D 2013-72.

4. Dennis, R., et al. Filtration Model for Coal Fly Ash with Glass Fabrics. GCA/Technology Division. EPA-600/7-77-084. August 1977.

5. Culbertson, W. J. Development of Standard Laboratory Resistivity Apparatus. Denver Research Institute. EPRI FP-885. August 1978.

6. Dennis, R., and H. A. Klemm. Fabric Filter Model Format Change: Volume I. Detailed Technical Report. GCA/Technology Division. EPA-600/7-79-043a. February 1979.

7. Dennis, R., and H. A. Klemm. Fabric Filter Model Format Change: Volume II. User's Guide. GCA/Technology Division. EPA-600/7-79-043b. February 1979.

8. Dennis, R., H. A. Klemm, and W. Battye. Fabric Filter Model Sensitivity Analysis. GCA/Technology Division. EPA-600/7-79-043c. April 1979.

9. McDonald, J. R. A Mathematical Model of Electrostatic Precipitation (Revision 1): Volume I. Modeling and Programming. Southern Research Institute. EPA-600/7-78-111a. June 1978.

10. McDonald, J. R. A Mathematical Model of Electrostatic Precipitation (Revision 1): Volume II. User Manual. Southern Research Institute. EPA-600/7-78-111b. June 1978.

11. Pope, Evans, and Robbins, Inc. Multicell Fluidized-Bed Boiler Design, Construction and Test Program. Research and Development Report No. 90, Interim Report No. 1 for Period October 1972-June 1974. Prepared for the U.S. Department of the Interior. PB 236 254. August 1974.

12. Shale, C. C., J. H. Holden, and G. E. Fasching. Electrical Resistivity of Fly Ash at Temperatures to 1500°F. U.S. Bureau of Mines Report. No. RI 7041.

13. Szabo, M. F., and R. W. Gerstle. Operation and Maintenance of Particulate Control Devices on Coal-Fired Utility Boilers. PEDCo Environmental, Inc. EPA-600/2-77-129. July 1977.

14. Billings, C. E., and J. Wilder. Handbook of Fabric Filter Technology. Volume I. Prepared by GCA/Technology Division for the National Air Pollution Control Administration, Contract No. CPA-22-69-38. December 1970.

15. Stenby, E. W., L. W. A. Bye, and R. J. Beaton. The Kramer Baghouse. In: Proceedings of the American Power Conference, Chicago, Illinois. April 23-25, 1979.

16. Electric Power Research Institute (EPRI). Test data reported in the PRECIP Newsletter, published by the McIlvaine Co., Northbrook, Illinois, Number 18. July 20, 1977.

17. Electric Power Research Institute (EPRI). Test data reported in the PRECIP Newsletter, published by the McIlvaine Co., Northbrook, Illinois, Number 21. October 20, 1977.

18. Gooch, J. P., and G. H. Marchant. Electrostatic Precipitator Rapping Reentrainment and Computer Model Studies. Southern Research Institute. EPRI FP-792, Volume 3. August 1978.

APPENDIX A

PARTICLE SIZE AND FILTRATION PARAMETER MEASUREMENTS

GENERAL DESCRIPTION

All particle size distribution and filtration parameter measurements for the five fly ash samples in this study were made using the GCA bench scale fabric filter test assembly.[1] This system is shown schematically in Figure A-1. Test aerosols are generated with a National Bureau of Standards (NBS) dust feeder.[2] In this device, dust falls from a small hopper onto a slowly rotating spur gear. A clean, dried compressed air stream of about 0.11 m^3/min (4 acfm) at 276 kPa (40 psig) entrains the dust through an aspirating tube and then redisperses the dust by the high velocity shearing action in the compressed air ejector nozzle. The total air flow produced by this system (compressed air plus aspirated air) is approximately 0.23 m^3/min (8 acfm).

The well-dispersed dust is injected into the duct as shown in Figure A-1. The aerosol sample for the test equipment is extracted isokinetically from this duct through a sampling probe attached to the filter system inlet pipe. Excess air and dust are vented to a waste gas treatment system. During testing, all components of the test system are electrically grounded to reduce the possibility of electrostatic particle losses and to minimize other potential electrostatic effects.

PARTICLE SIZE ANALYSES

The particle size distribution for each redispersed fly ash was measured with an Andersen Mark III (eight-stage) Stack Sampler (Andersen 2000 Inc., Atlanta, GA) equipped with pre-weighed glass fiber collection substrates and a pre-weighed backup filter. The Andersen Mark III impactor is shown in Figure A-2. The impactor inlet was modified by attaching a straight 25 cm (10 in.) long, 0.8 cm (0.3 in.) i.d. probe to the inlet cone, in place of the nozzle shown in Figure A-2. With this arrangement, the impactor could be mounted vertically above the inlet manifold in Figure A-1. In order to extract a representative fly ash sample for particle sizing, the impactor probe inlet was located opposite the center of the fabric panel.

Impactor flow rates were set at approximately 0.014 m^3/min (0.50 acfm), the nominal rate for the Andersen Mark III impactor. Instantaneous and cumulative flow measurements were made with a calibrated orifice meter and a dry test meter, respectively.

Because particle size analysis and filtration tests could not be run simultaneously, certain precautions were taken to ensure that equivalent samples were extracted during both types of tests. The sampling probe to the

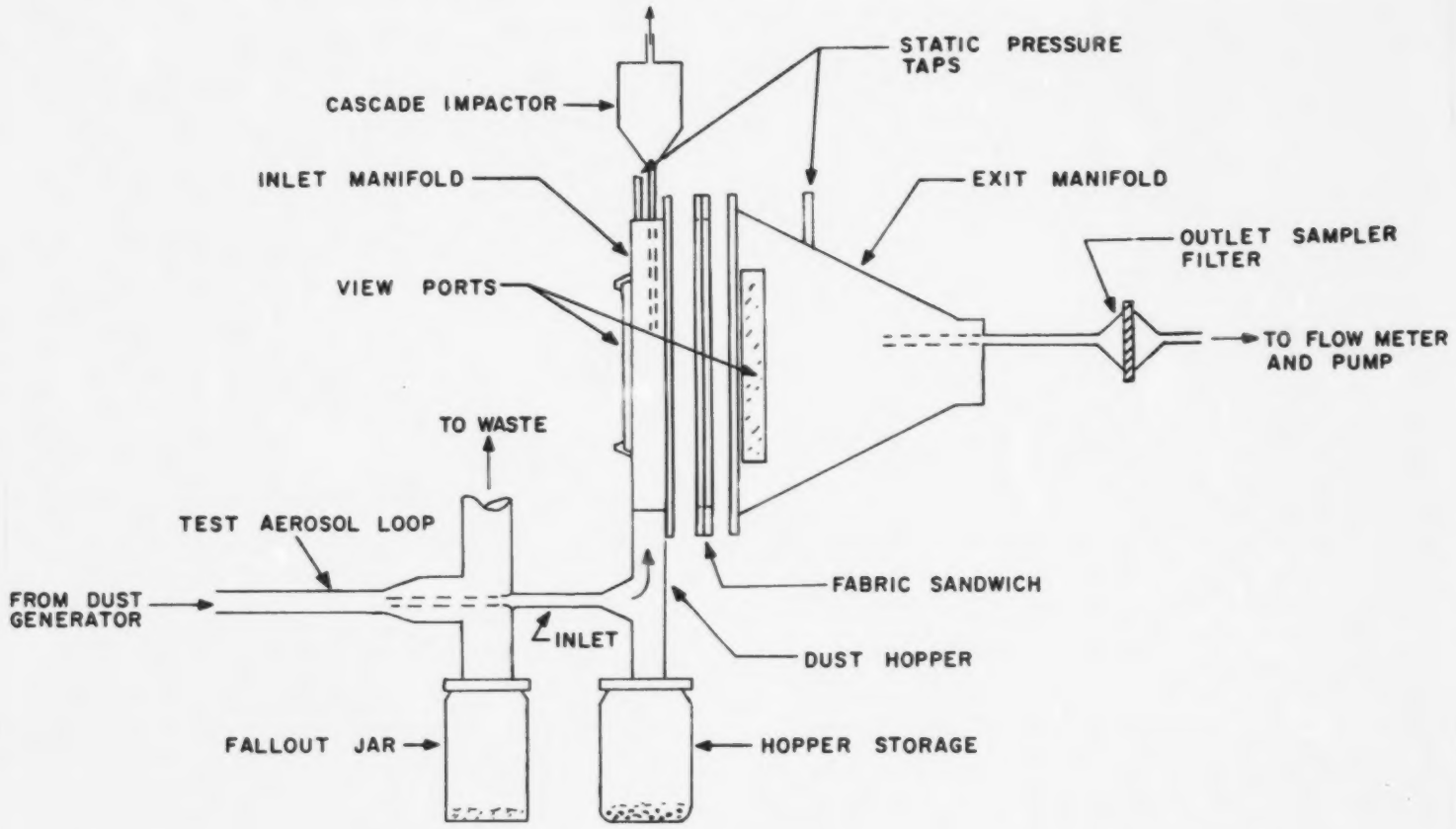

Figure A-1. GCA bench scale fabric filter test assembly.

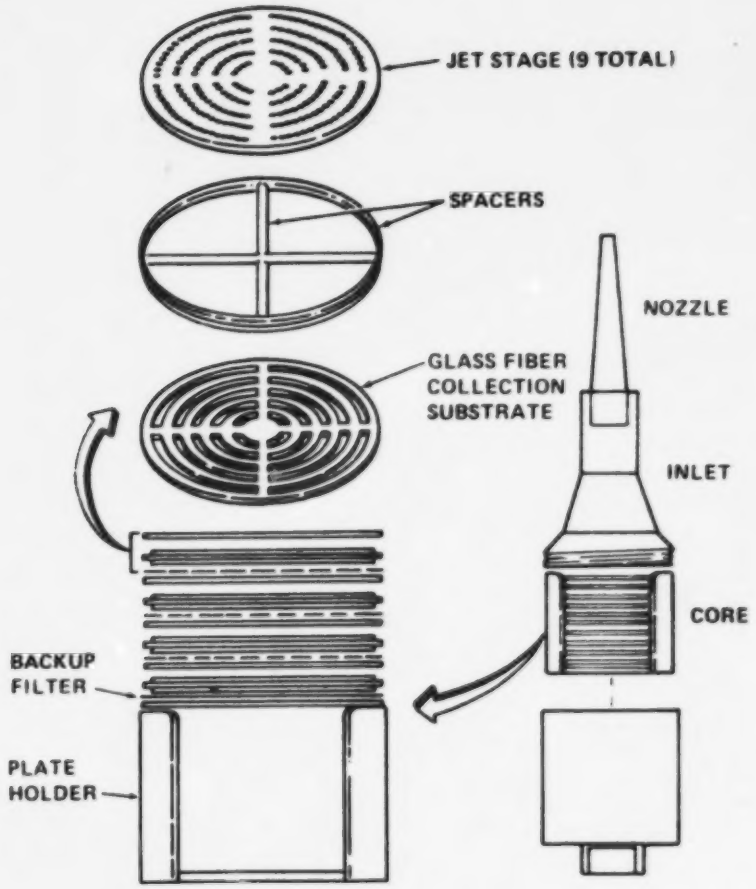

Figure A-2. Andersen Mark III Stack Sampler.

test aerosol loop in Figure A-1 was identical in both cases. However, the air flow required for filtration tests (see below) was nearly twice the nominal flow rate of the impactor. To compensate for this, an additional air flow of 0.014 m^3/min (0.50 acfm) was drawn into the test system during particle size measurement tests. This additional flow, necessary to maintain isokinetic extraction conditions from the test aerosol loop, was pulled through the fabric panel by a second pump. A critical orifice was used to provide a constant air flow.

Two impactor samples were taken for each fly ash. Because the inlet concentrations averaged 1.5 g/m^3 (0.66 grains/acfm), sampling times were limited to 1 to 2 minutes. A visual inspection of the fly ash deposited on the collection substrates during the first sample was used to adjust the time of the second sample accordingly.

Standard procedures[3,4] for impactor cleanup were followed. All substrates and filters were weighed (along with blanks) to 0.01 mg on a Mettler balance. Constant weights, to within 0.1 mg, were recorded for subsequent calculations. The manufacturer's calibration data for stage jet diameters and for the inertial impaction parameter ($\sqrt{\psi}$) were used to calculate cut diameters (diameter of the particle that is collected with 50 percent efficiency) for each impactor stage. An iterative procedure, adapted for a programmable pocket calculator,[5] was used for these calculations.

Cumulative particle size distributions were plotted on log-probability paper for the two impactor sizings performed for each fly ash. A straight line was fitted by eye to each plot and values for aerodynamic mass median diameter (aMMD) and geometric standard deviation (σ_g) were obtained from the line. These cumulative size distribution curves for the five resuspended FBC fly ash samples are shown in Figures A-3 through A-7.

FILTRATION TESTS

A series of tests was run to determine the specific resistance coefficient (K_2) for each of the five FBC fly ash samples. K_2 is a measure of the filterability of a dust on a fabric surface. More specifically, K_2 describes the linear increase in drag (pressure loss across the filter divided by the gas velocity through the filter) that occurs as a dust layer on the fabric increases uniformly in thickness.

To measure K_2, each resuspended fly ash was filtered through a 15 cm x 23 cm (6 in. x 9 in.) panel of fiberglass fabric with a 10 percent Teflon B coating (Menardi-Southern, Division of United States Filter Corporation, Style 601 TUFLEX). Teflon-coated fiberglass fabrics are commonly used in fabric filter collectors applied to conventional coal-fired utility and industrial boilers. A new fabric panel used for the initial test was subsequently cleaned and reused for later tests. The fabric panel was supported in a rigid metal frame. This allowed the panel to be removed from the test system periodically for weighing without disturbing the accumulated dust layer.

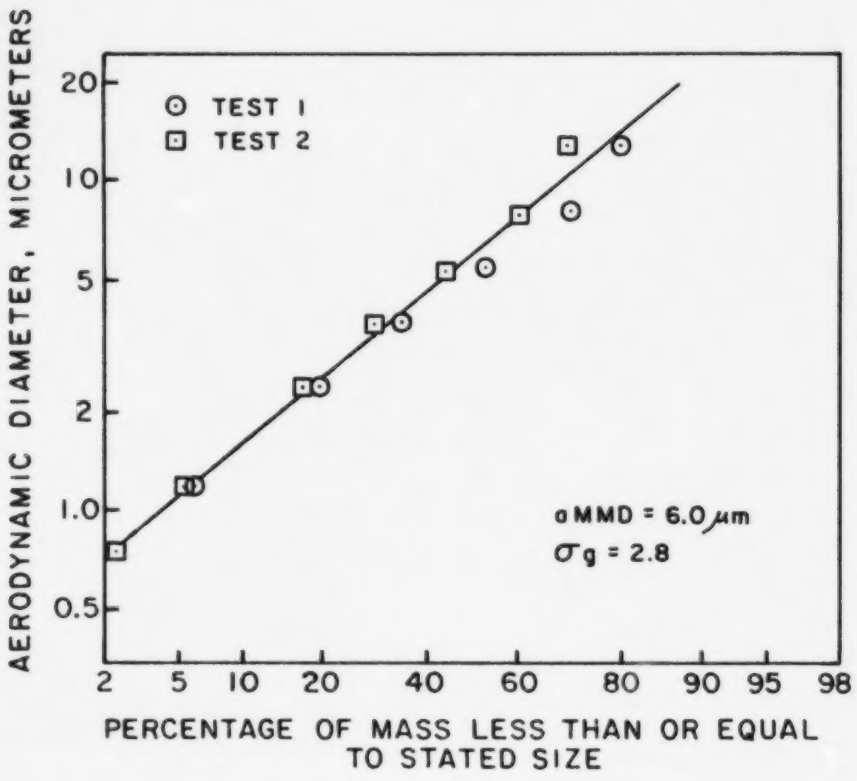

Figure A-3. Particle size distribution for Sample A (Alliance) resuspended fly ash, Andersen Mark III impactor measurements.

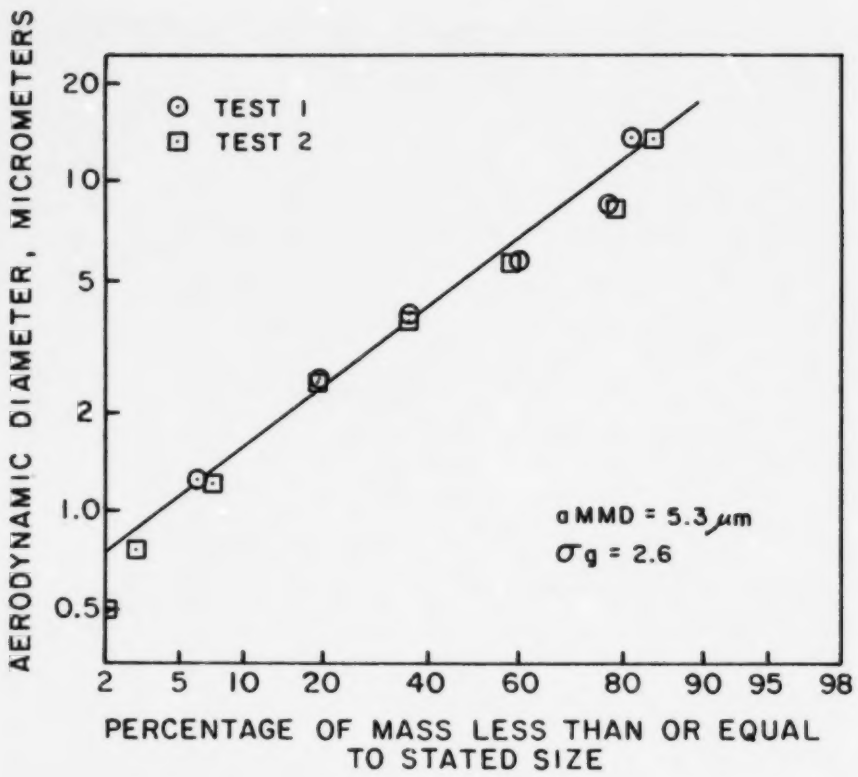

Figure A-4. Particle size distribution for Sample B (SATR) resuspended fly ash, Andersen Mark III impactor measurements.

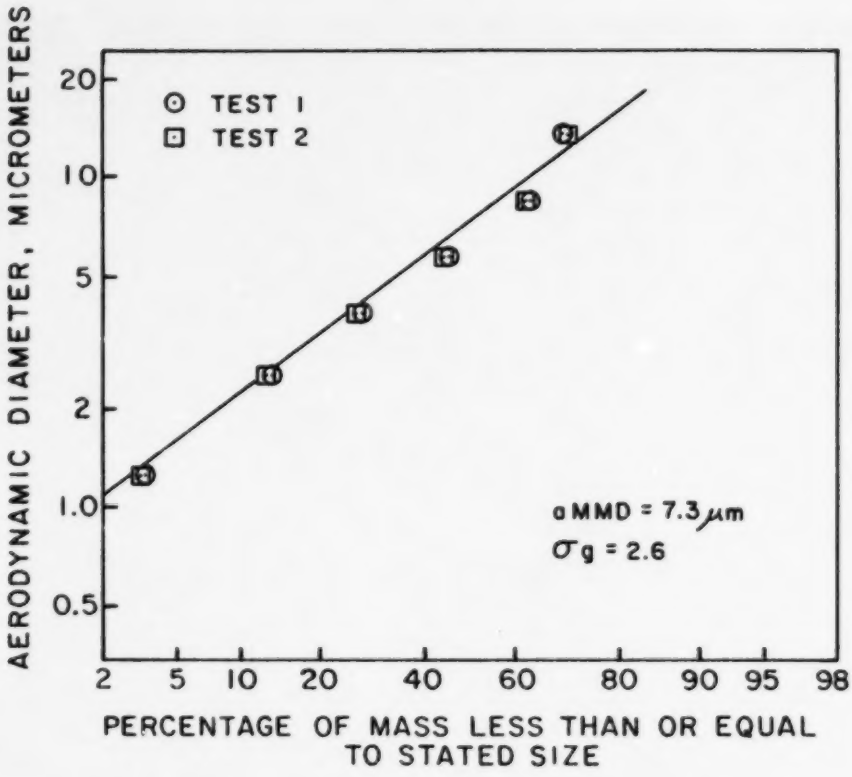

Figure A-5. Particle size distribution for Sample C (FluiDyne without fly ash recycle) resuspended fly ash, Andersen Mark III impactor measurements.

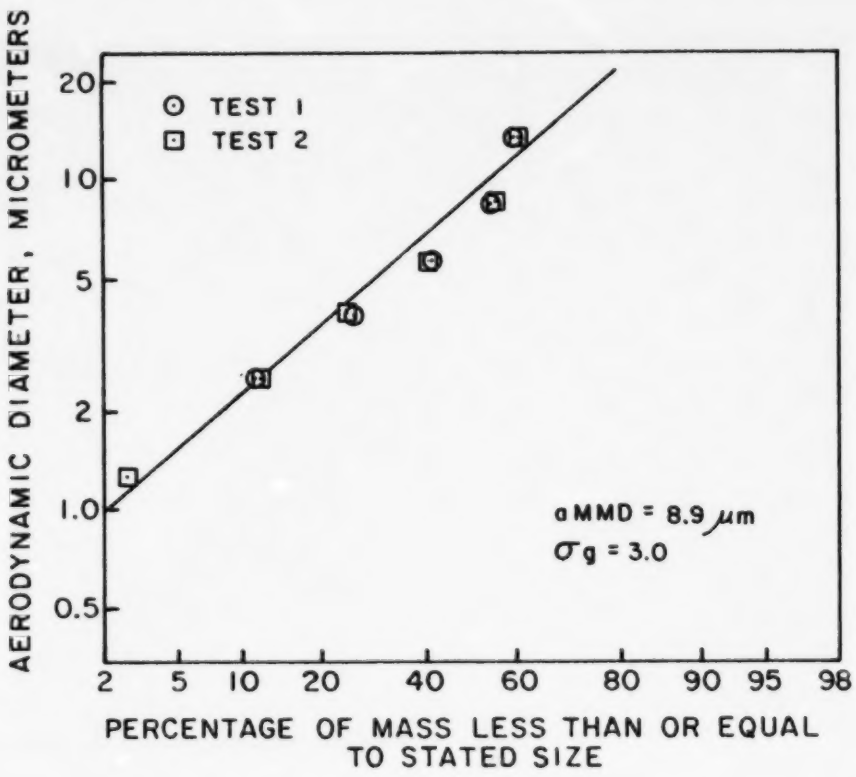

Figure A-6. Particle size distribution for Sample D (FluiDyne with fly ash recycle) resuspended fly ash, Andersen Mark III impactor measurements.

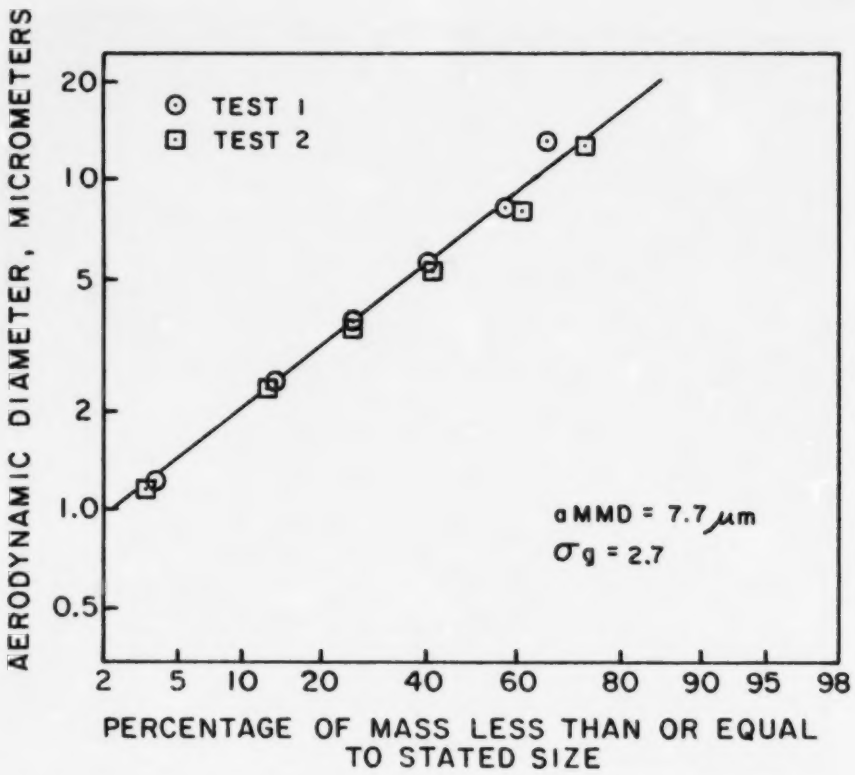

Figure A-7. Particle size distribution for Sample E (Georgetown) resuspended fly ash, Andersen Mark III impactor measurements.

All filtration tests were carried out at an air-to-cloth ratio (volume flow through the fabric filter divided by the fabric surface area) of 0.76 m/min (2.5 ft/min). This value is typical of the air-to-cloth ratios of fabric filter collectors that are cleaned by reverse air or mechanical shaking. Instantaneous air flow through the filter was monitored with an orifice meter while the total volume of air filtered was recorded by a dry test meter and corrected to pressure and temperature conditions at the fabric surface.

The test procedure consisted of the following steps. Prior to each test, the fabric panel was weighed to determine its residual dust loading after cleaning. The test system was then assembled and filtration was carried out for a period of 1 to 2 hours. During the filtration period, the pressure loss across the fabric filter was recorded at 5-minute intervals. Static pressure taps on the upstream and downstream sides of the filter (shown in Figure A-1) were used to make these measurements. At the end of each filtration period, the fabric panel was reweighed to determine the mass of fly ash collected. For each of the five FBC fly ashes, the K_2 measurement consisted of two or more consecutive filtration periods. Final fabric dust loadings ranged from approximately 230 to 370 g/m^2 (0.047 to 0.076 lb/ft^2).

Curves of filter drag versus dust loading were constructed from the data collected. The open circles in Figures A-8 through A-12 represent actual filter weighings at the beginning and end points of each filtration period. By assuming that the inlet fly ash concentration remained constant, it was possible to calculate intermediate dust loadings corresponding to the pressure loss measurements made during the filtration period. These points are indicated by the closed circles in Figures A-8 through A-12.

For the purpose of estimating K_2, the initial portion of the drag versus dust loading curve was ignored. This region is characteristic of filtration by new or cleaned woven fabrics. The rapid increase in drag occurs as pores formed at the junctures of the warp and fill yarns of the fabric are filled during the early stages of filtration. After these pores or depressions have been filled, the curve of drag versus dust loading assumes a more linear form.

The measured drag and dust loading values for the filtration period end points plus the drag and estimated dust loading value at the point where the curve becomes essentially linear were fitted to a straight line by the method of least squares. The slope of this line provided the estimate of the specific resistance coefficient, K_2, for each fly ash. Even though all five curves appear slightly curvilinear (possibly due to compression of the dust layer and/or fabric during filtration), a linear approximation provided a reasonable K_2 estimate. The minimum coefficient of correlation (r) obtained by the linear regression estimation method was 0.99.

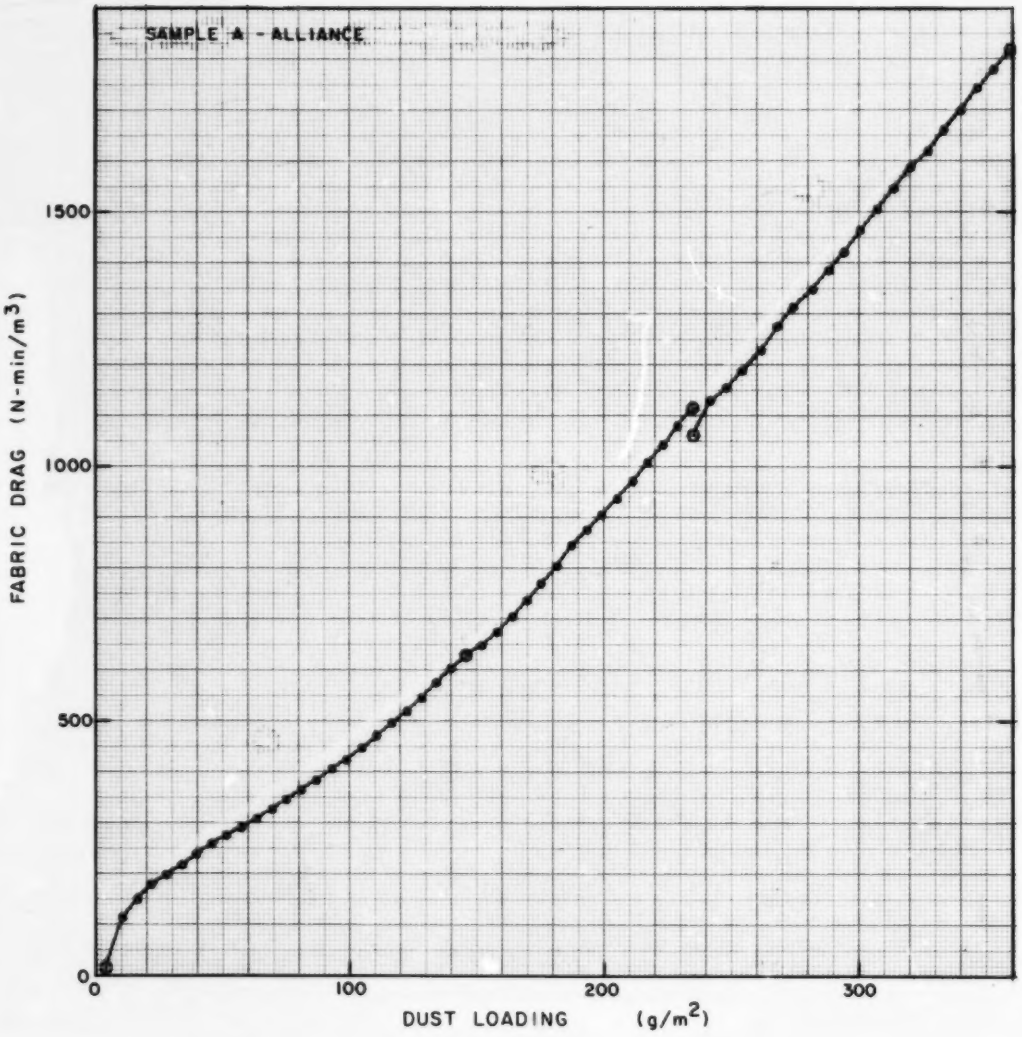

Figure A-8. Drag versus dust loading curve for Teflon-coated fiberglass fabric and Sample A (Alliance) resuspended fly ash.

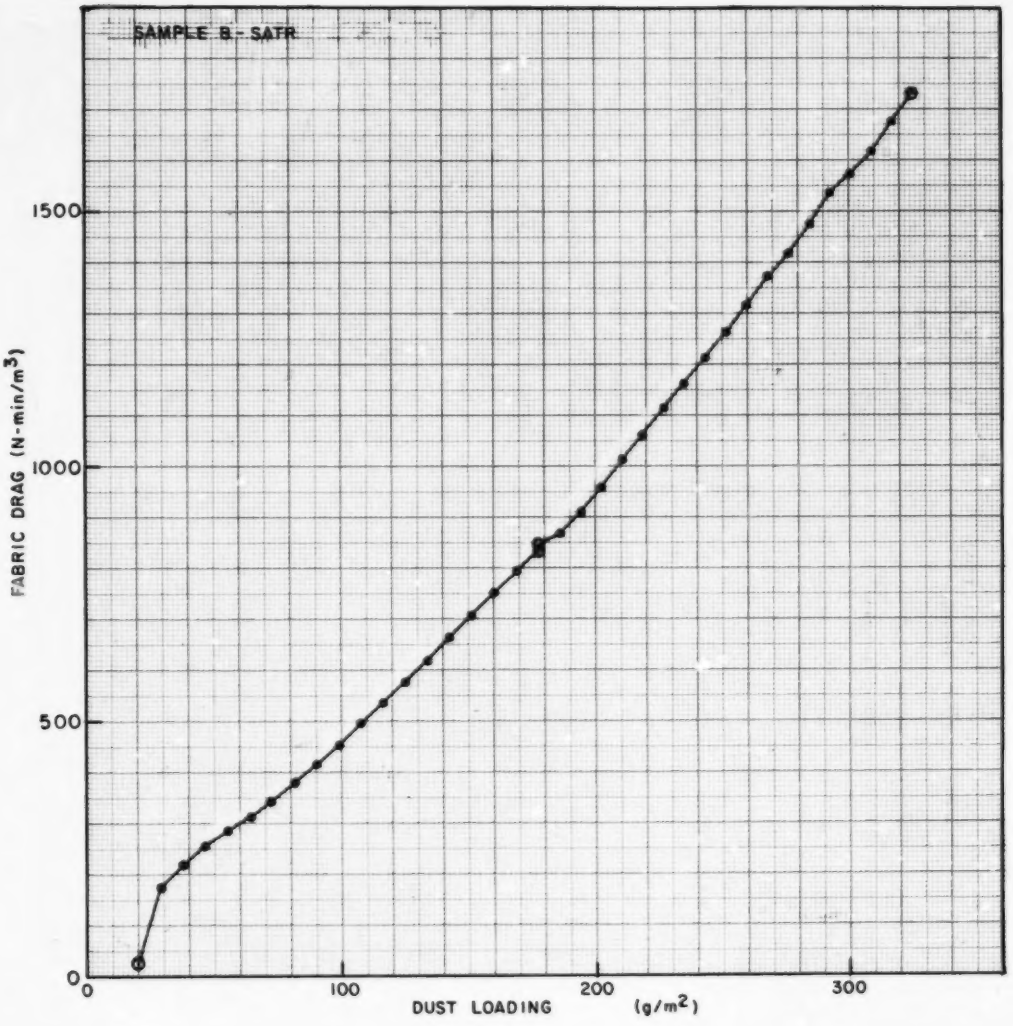

Figure A-9. Drag versus dust loading curve for Teflon-coated fiberglass fabric and Sample B (SATR) resuspended fly ash.

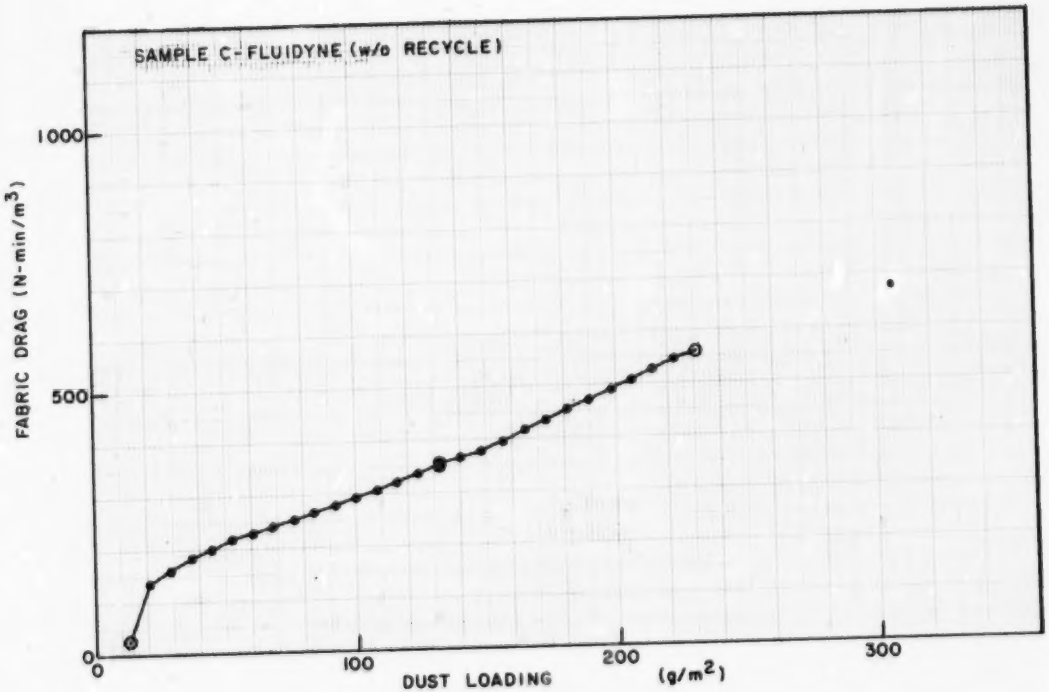

Figure A-10. Drag versus dust loading curve for Teflon-coated fiberglass fabric and Sample C (FluiDyne without recycle) resuspended fly ash.

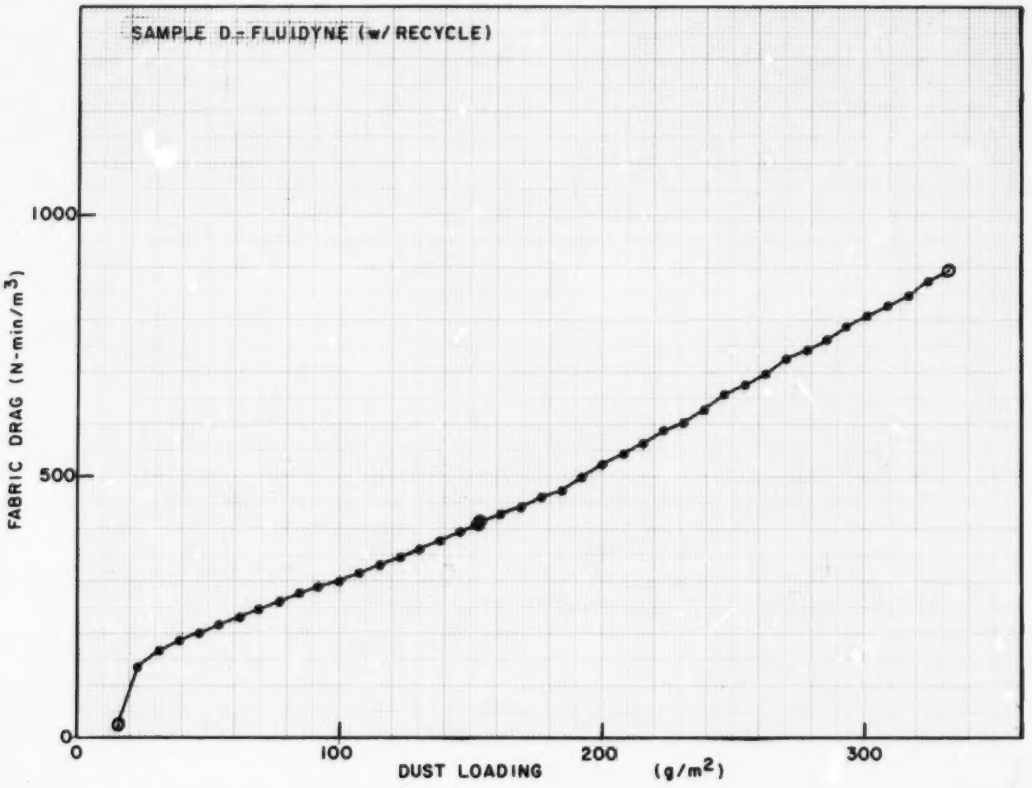

Figure A-11. Drag versus dust loading curve for Teflon-coated fiberglass fabric and Sample D (FluiDyne with recycle) resuspended fly ash.

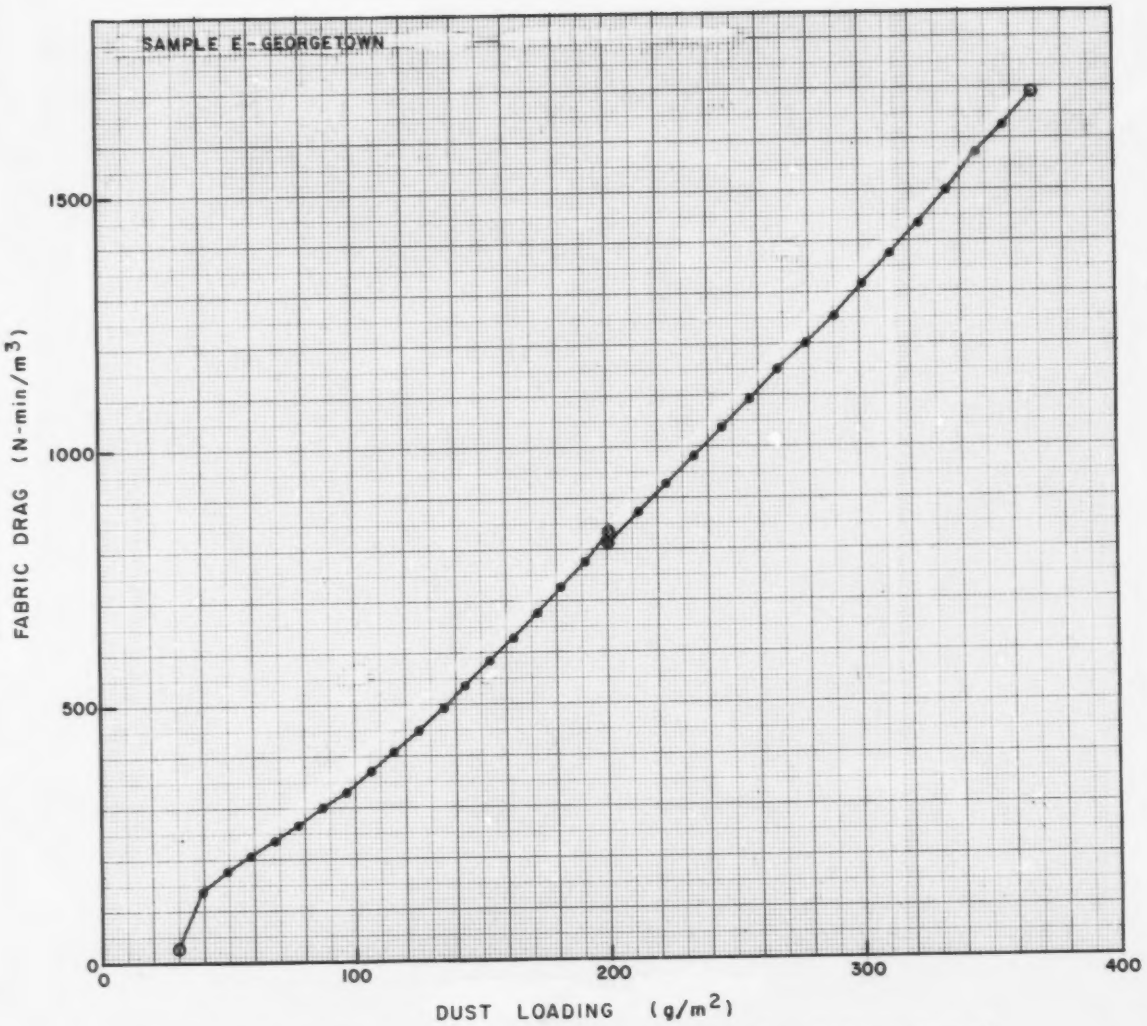

Figure A-12. Drag versus dust loading curve for Teflon-coated fiberglass fabric and Sample E (Georgetown) resuspended fly ash.

REFERENCES FOR APPENDIX A

1. Dennis, R., et al. Filtration Model for Coal Fly Ash with Glass Fabrics. GCA/Technology Division. EPA-600/7-77-084. August 1977.

2. Dill, R. S. A Test Method for Air Filters. Trans. Amer. Soc. Heat Vent. Eng. 44:379. 1938.

3. Andersen 2000 Inc. Operating Manual for Andersen 2000 Inc. Mark II and Mark III Particle Sizing Stack Samplers. Revision A, TR # 76-900023. August 1, 1977.

4. Cushing, K. M., and W. B. Smith. Procedures Manual for Fabric Filter Evaluation. Southern Research Institute. EPA-600/7-78-113. June 1978.

5. Ragland, J. W., et al. HP-25 Programmable Pocket Calculator Applied to Air Pollution Measurement Studies: Stationary Sources. Southern Research Institute. EPA-600/7-77-058. June 1977.

APPENDIX B

RESISTIVITY MEASUREMENTS

Laboratory resistivity measurements were conducted by Denver Research Institute (DRI) for each of the five hopper fly ash samples taken from fabric filters servicing four atmospheric fluidized-bed combustion units. (Samples D and C were taken from the same system; with and without fly ash recycle respectively.)

Developed by DRI, the resistivity measurement system consists of several resistivity cells and an automated data collection system. Figure B-1 is an overall view of the apparatus with the Data General Nova Model 4001 general purpose minicomputer on the left and the temperature-controlled oven on the right.[1] The Nova computer controls the system and the operator controls the computer through the teletype. Values for voltage, temperature, humidity and the geometry and electrical data for the resistivity cells can be entered at the keyboard or using a prerecorded program via the cassette tape drive.

The voltage that is applied to the cells is controlled by the computer through the multichannel D/A (digital-to-analog) converter and logic circuit. This converter in conjunction with programmable power supplies (0-15 kV output) and a programmable temperature controller allows direct control of voltage and temperature.

Figure B-2 is a view of the open oven with the parallel plate cells in position.[1] Each cell consists essentially of two parallel stainless steel fritted disks contained in a Coors Al_2O_3 cup. The cell is loaded with fly ash by removing the top frit and plug, pouring in the desired amount, and then replacing the plug, which attaches to the upper disk electrode. The weight spreads and compacts the ash to a relatively constant density. Since the plug is flush with the top of the Coors insulating tube when the cell is empty, the depth of the fly ash in the cell is equal to the difference in height of the two pieces which is measured by a micrometer.

In order to minimize temperature gradients in the oven and to raise the cell temperature quickly, a fan circulates the heated air over the cells. Simulated flue gas, nitrogen or air, is drawn through three temperature controlled fritted glass water bubblers in order to control humidity before entering a heated manifold. The gases are then directed over both sides of each cell so that they will diffuse into the ash sample from both sides. These gases are then exhausted to the atmosphere.

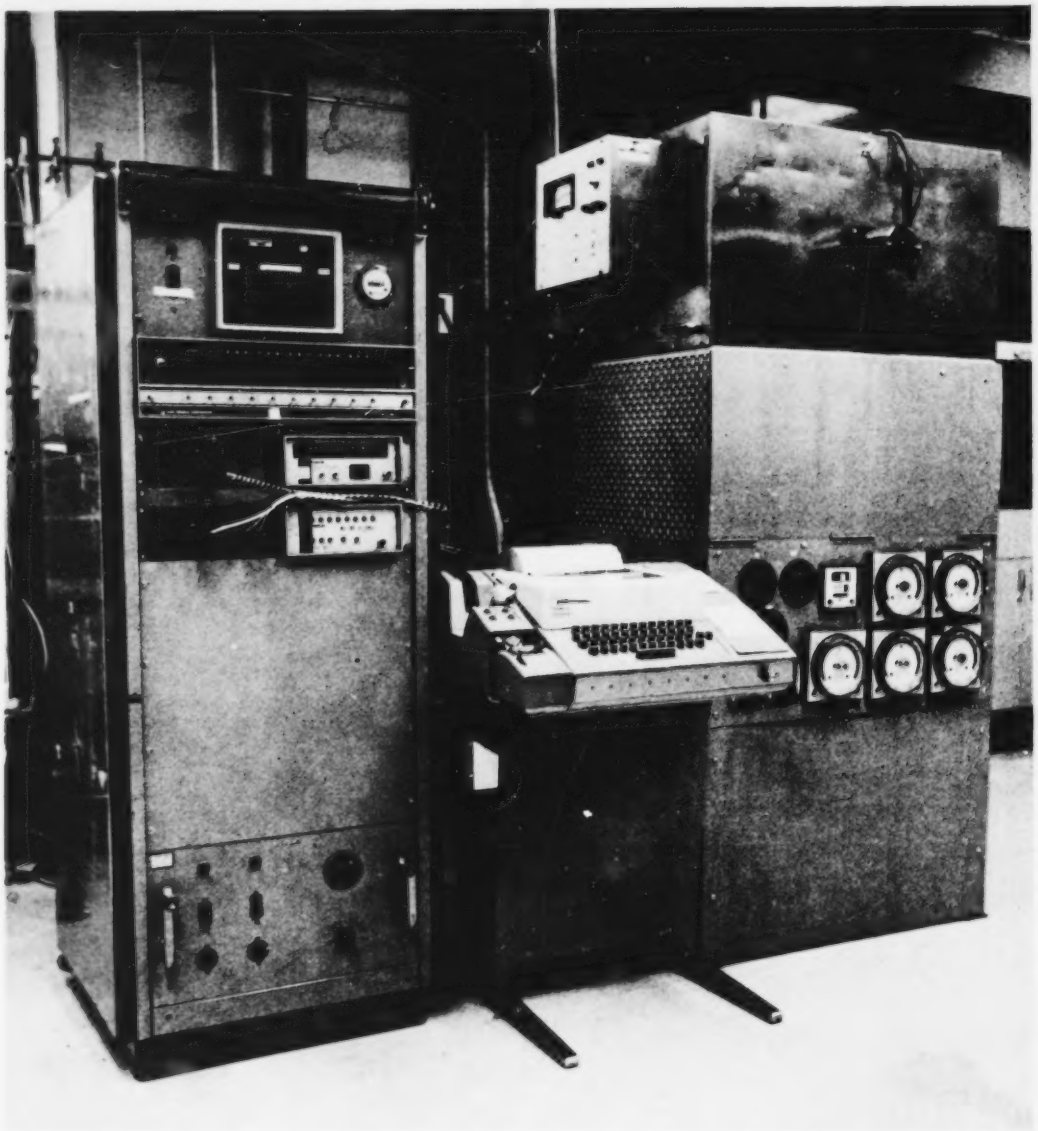

Figure B-1. Overall view of computer and resistivity apparatus.[1]

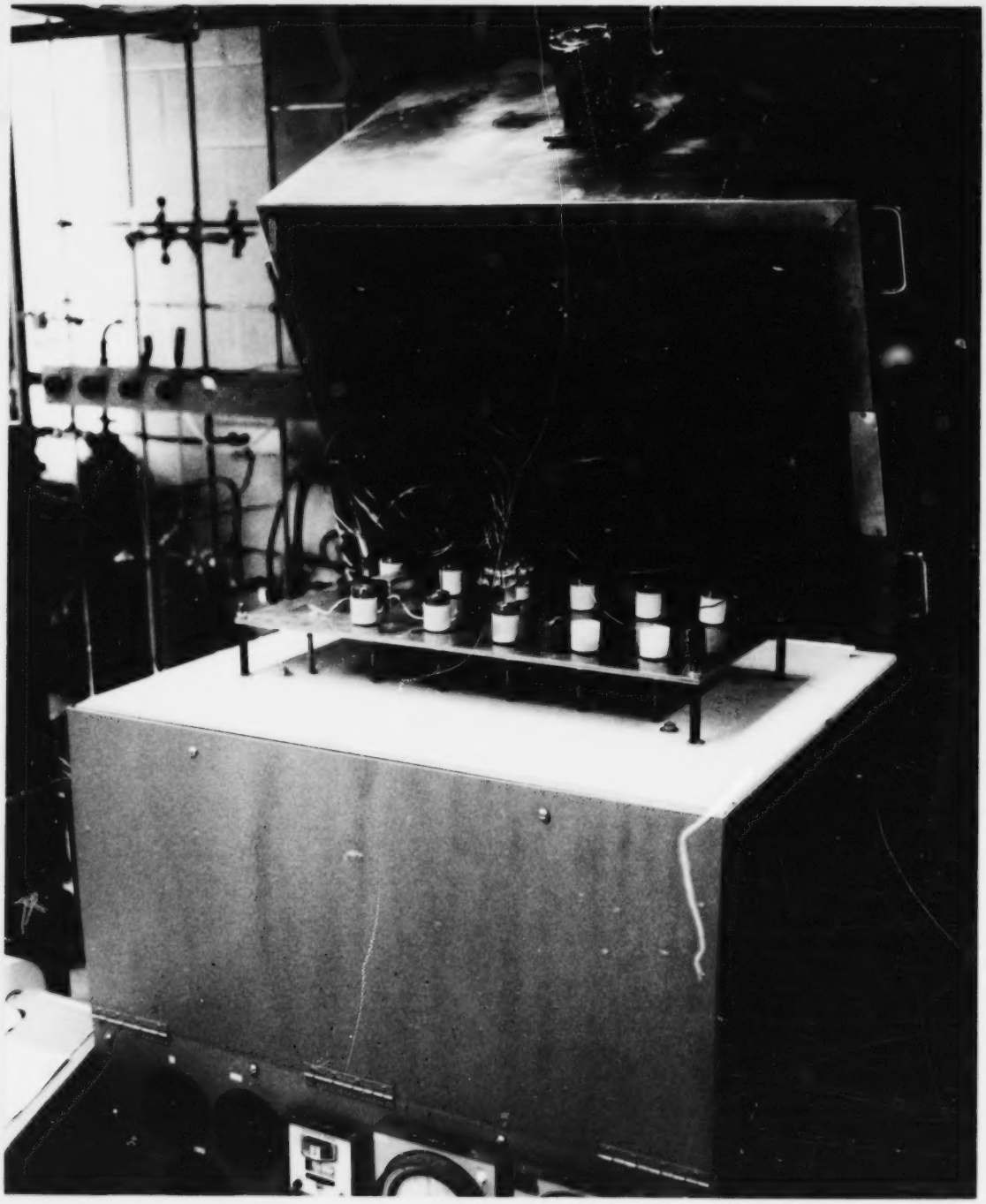

Figure B-2. Open oven showing parallel plate unguarded cells.[1]

MULTIPLE CELL OPERATION

Using the computer-controlled system discussed above, resistivity versus temperature plots were developed for samples B, C, and D as shown in Figures B-3, B-4, and B-5 respectively. Sample A, which was also tested at this time and exhibited the darkest color of the four samples, "tripped out" the computer during the first run. This is generally indicative of a low resistivity ash often caused by high carbon content in the ash as suggested by its dark color. Sample A was subsequently removed from its cell and the test continued through the temperature range of 120-370°C (250-700°F) for samples B, C, and D. Upon retesting, sample A showed sporatic readings, indicating that the actual resistivity was below the detection limits of the apparatus; i.e., below 10^7 ohm-cm.

SINGLE CELL OPERATION

Both samples A and E, whose resistivity versus temperature plots are shown in Figures B-6 and B-7, were tested in one single cell unit because of the low resistivity encountered when a preliminary test was conducted on the computer-controlled system. The single cell apparatus is manually operated and uses a 1.5 kV, 5 mA power supply, which allows resistivities as low as 10^3 ohm-cm to be measured. Both samples sparked over at 260°C (500°F), which precluded any further testing. This was attributed to the high carbon content of these two samples.

EFFECT OF CARBON CONTENT ON RESISTIVITY

In independent tests conducted by Denver Research Institute to ascertain the effect of carbon content of fly ash on resistivity, high carbon content fine ash from a stoker boiler was added to fly ash samples from one of the Four Corners power stations in New Mexico.[1] Within the range of 120-370°C (250-700°F) and 0 to 20 percent humidity, the resistivity of ash mixtures containing 1, 2, and 5 percent total carbon resulted in less than a 15 percent variation. Specifically, when the carbon content was increased to 10 percent by weight, the resistivity decreased by a factor of approximately 100. At 20 percent carbon content, the resistivity decreased by a factor of approximately 1000.

Although no quantitative correlations were developed from the resistivity and carbon content measurements of the five FBC fly ash samples, it was noted that resistivity varied inversely with carbon content. For conventionally generated fly ash, carbon contents above 8 to 10 percent have been found to be a critical factor in decreasing resistivity.[2] The results shown in Figure 6 (in the text) suggest that resistivity of FBC fly ash is substantially reduced when the carbon content is above 20 percent by weight. Under these conditions, considerable sparkover in an electrostatic precipitator may occur.

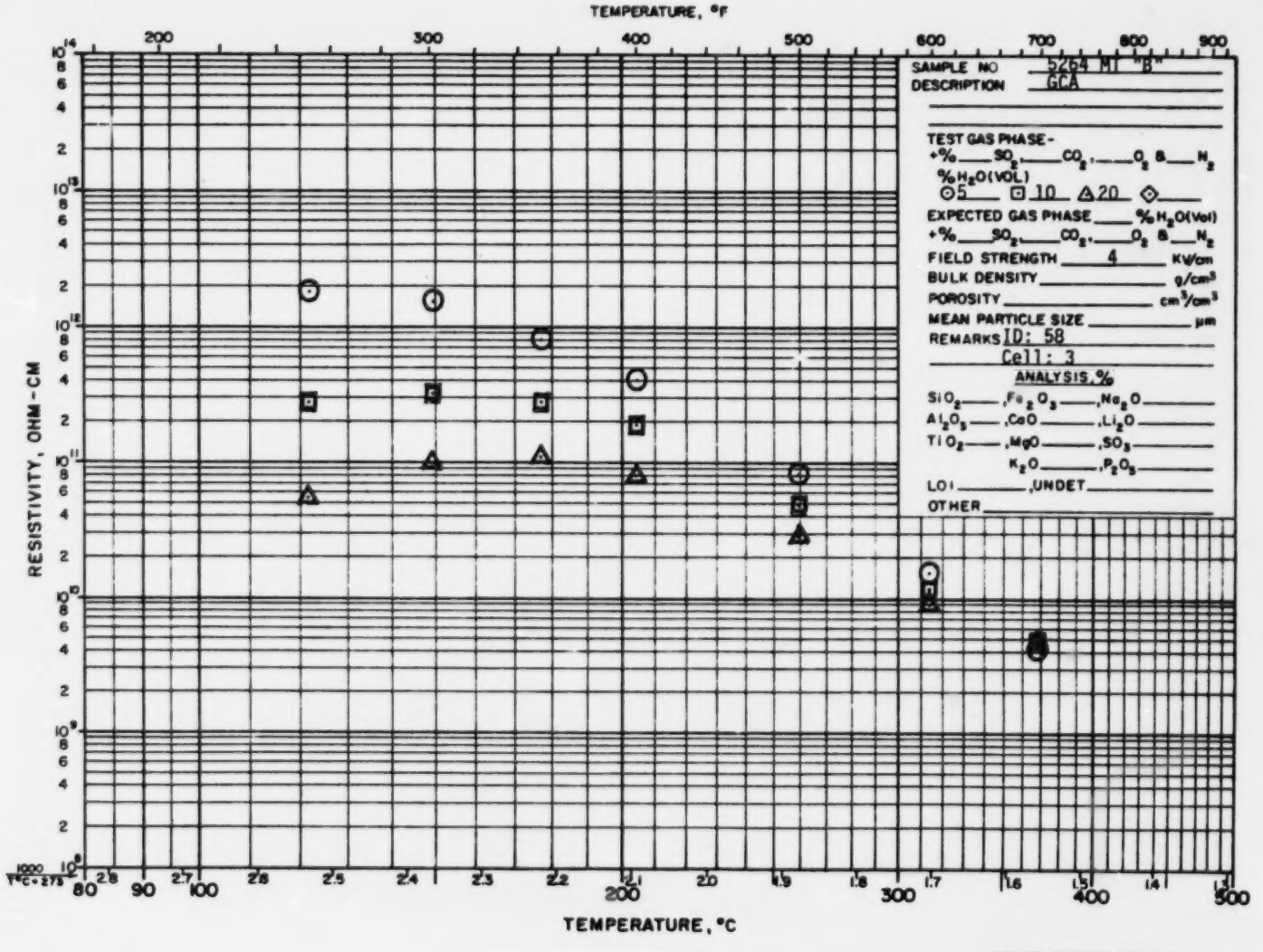

Figure B-3. Laboratory resistivity measurements versus temperature for fly ash Sample B (SATR).

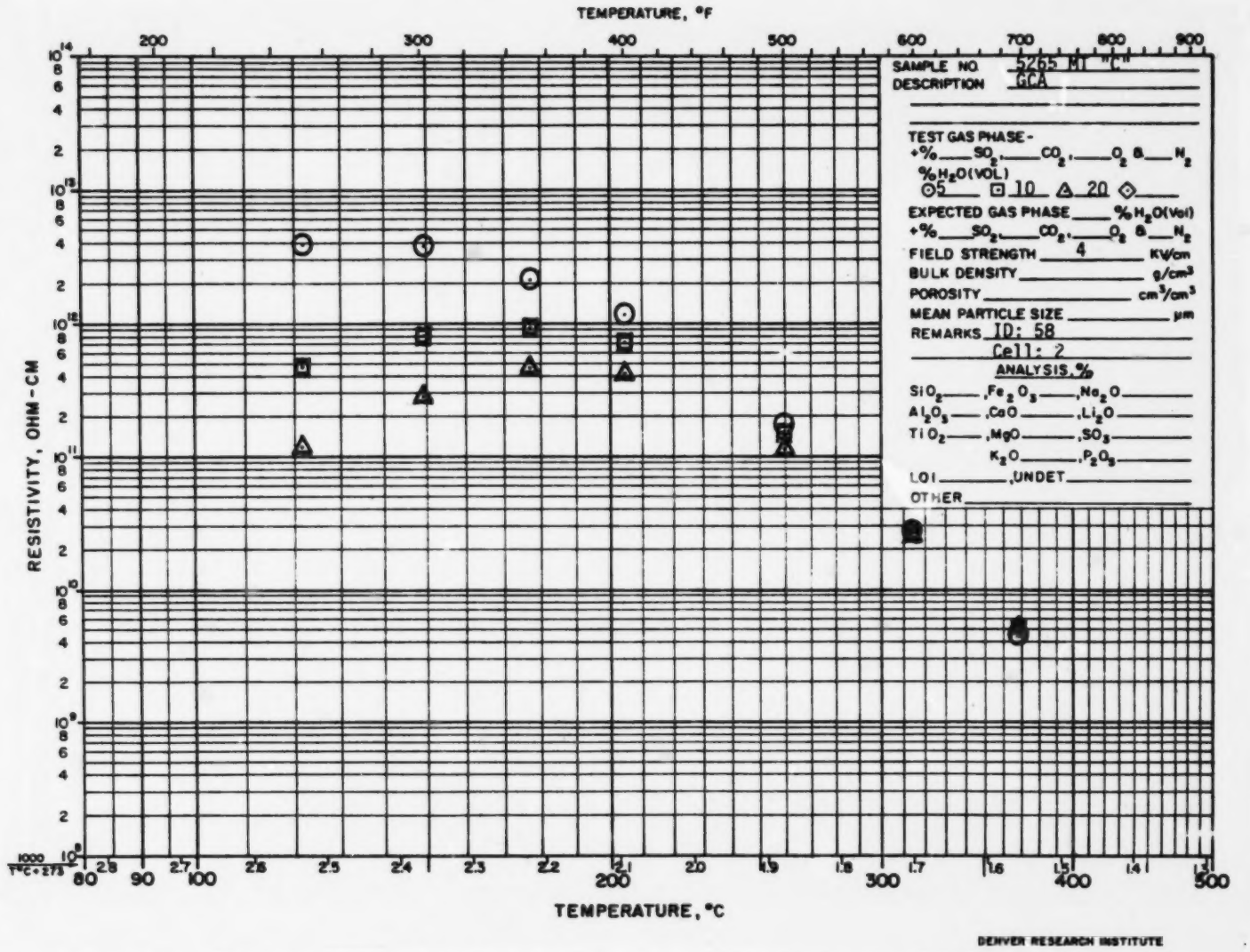

Figure B-4. Laboratory resistivity measurements versus temperature for fly ash Sample C (FluiDyne--without fly ash recycle).

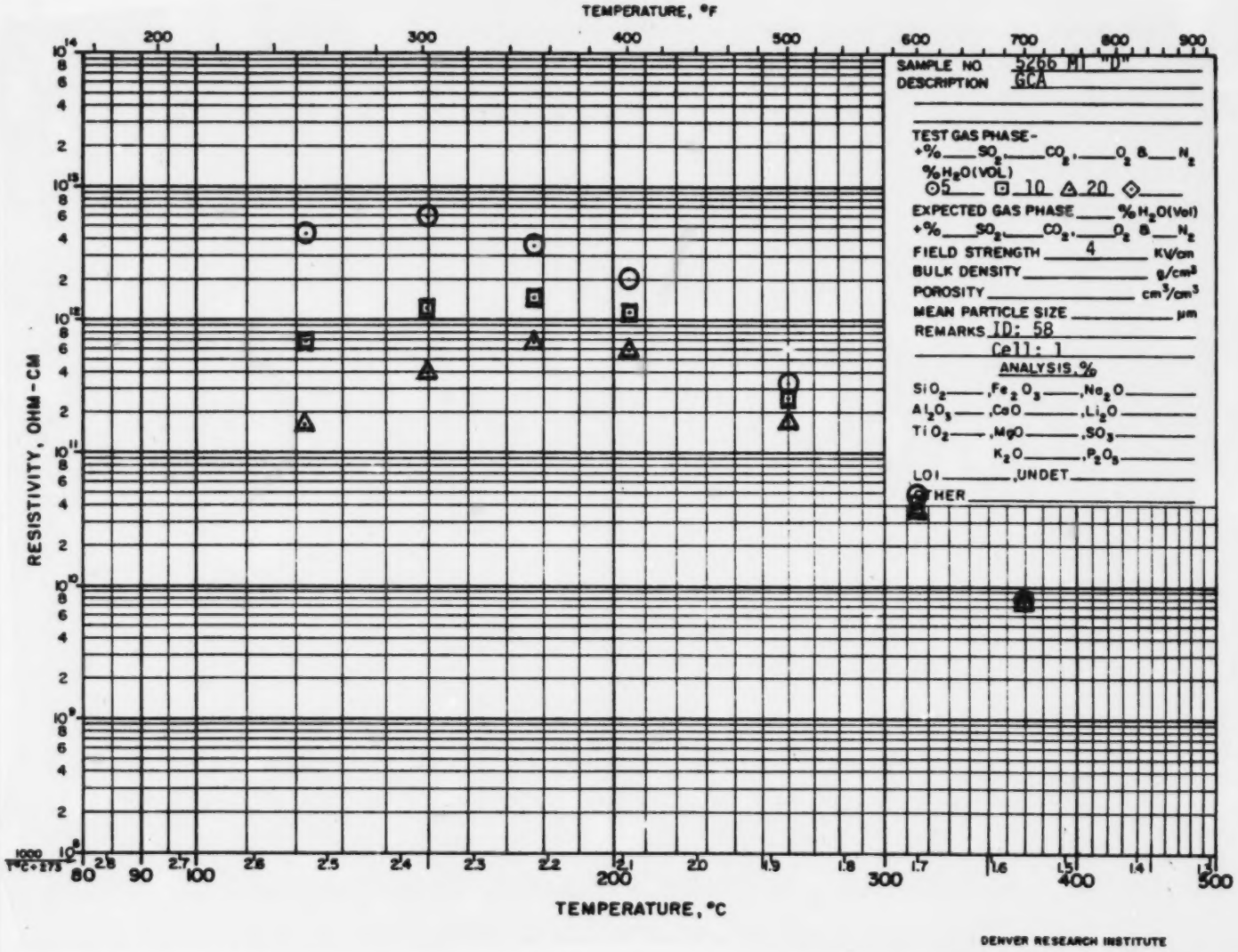

Figure B-5. Laboratory resistivity measurements versus temperature for fly ash Sample D (FluiDyne--with fly ash recycle).

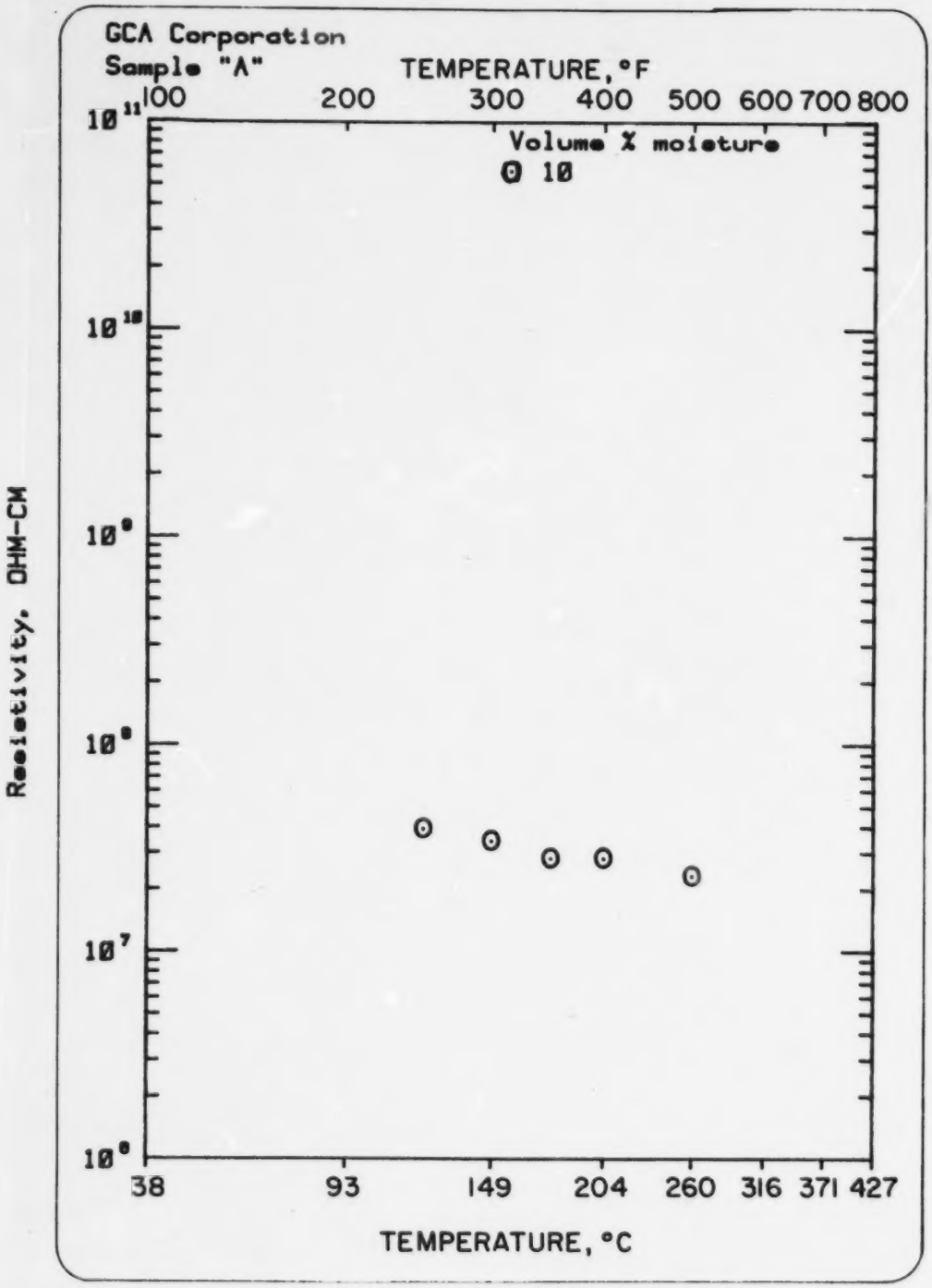

Figure B-6. Laboratory resistivity measurements versus temperature for fly ash Sample A (Alliance).

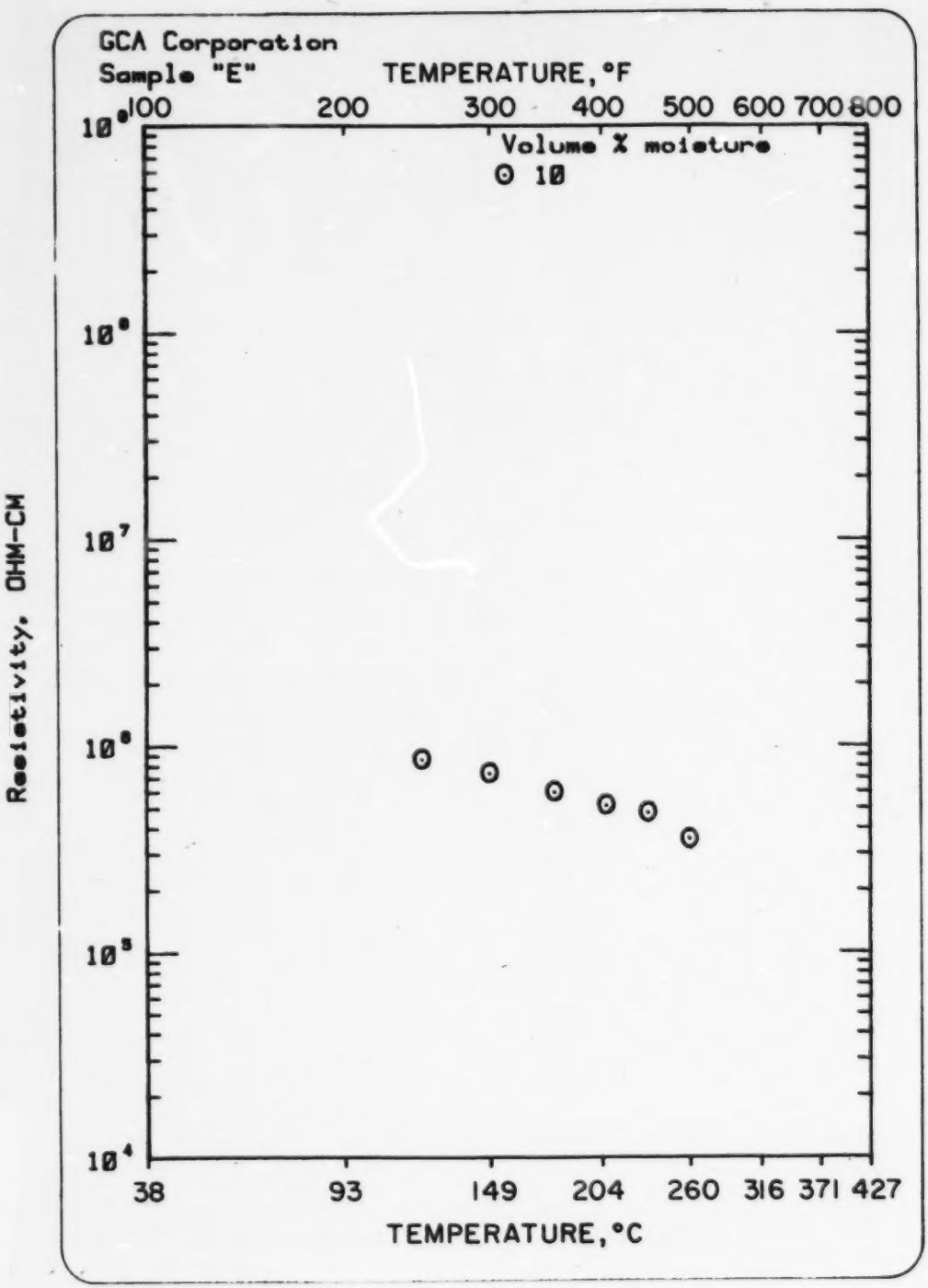

Figure B-7. Laboratory resistivity measurements versus temperature for fly ash Sample E (Georgetown).

REFERENCES FOR APPENDIX B

1. Culbertson, W. J., T. Espinoza, G. A. Rinard, and T. D. Nevens. Development of Standard Laboratory Resistivity Apparatus. Denver Research Institute. EPRI FP-885. August 1978.

2. Shale, C. C., J. H. Holden, and G. E. Fasching. Electrical Resistivity of Fly Ash at Temperatures to 1500°F. U.S. Bureau of Mines Report. No. RI 7041.

APPENDIX C

MORPHOLOGY CHARACTERIZATION AND CHEMICAL/SPECTRAL ANALYSIS

SCANNING ELECTRON MICROSCOPY EQUIPMENT

For the analysis of FBC fly ash samples, an Amray Model 1200 B scanning electron microscope (SEM) was used. Integrated with the SEM is a Kevex energy dispersive X-ray analysis (EDXRA) unit for quantitative and qualitative elemental analysis of fly ash particles. The guaranteed resolution limit of the microscope is 100 Å, but for routine analyses a 300-500 Å limit is more realistic. Polaroid photographs of the viewing screen can be taken at any magnification up to 100,000X, but most photomicrographs are taken between 50X and 20,000X. With the SEM, information on particle shapes, relative sizes, surface irregularities and impurities, textures, and topography is easily obtained. Combined with EDXRA the SEM becomes a tool that makes chemical analysis of particulate samples extremely rapid and accurate.

Energy dispersive X-ray analysis works on the principle of measuring the energy of the X-rays emitted by a particle when that particle is excited by an electron beam. The emitted radiation is collected by a lithium-drifted silicon detector which emits an electrical signal of an amplitude proportional to the incident X-ray radiation energy. The signal is then sorted and analyzed by a multichannel analyzer before being displayed as a typical X-ray spectrum on a cathode ray tube (CRT). The system detects X-ray energies simultaneously for all elements above nitrogen (atomic number 7).

Generally, the position of an element's X-ray energy peak is related to its atomic number and the height of the peak is weakly related to the amount present. However, since some elements, such as silicon, are more efficiently excited, they show a stronger or higher peak even though they may not be very abundant. To produce a quantitative analysis of the X-ray spectrum, a computer is used.

First, all background noise or white radiation produced from secondary X-ray emission is eliminated along with any edge absorption and spurious escape peaks not associated with any particular element. One is then left with a net count of X-ray emissions produced by elements present. Knowing the excitation efficiencies of each element, the computer corrects the heights of each elemental peak to represent actual abundancies. The results are then normalized to an abundance of 100 percent and printed out or displayed either as elemental metals or as oxides. Oxygen content and oxide abundancies are determined stoichiometrically.

Carbon, because of its low atomic number, is not readily detected by EDXRA. Therefore, the carbon content of each fly ash sample was determined by two alternate techniques, loss on ignition (LOI) analysis and a carbon-hydrogen-nitrogen (CHN) test. These methods are described in the main text. The abundancies of other elements in the samples were then readjusted downward after taking into account the carbon content of each fly ash. It is these EDXRA results, corrected for carbon content, which appear in Table 5 of the text.

SAMPLE PREPARATION

For SEM analysis and EDXRA, only a small sample is required (approximately 1 mg which is spread over a viewing area of one square centimeter). The SEM mounting stub, with double-sided adhesive tape on its surface, is pressed into the particulate sample, thereby coating the adhesive tape surface with enough particulate for a representative analysis. The SEM stub with the attached particulate is then placed into a sputtering unit to uniformly coat the particulate material and stub with approximately 100 Å of gold and palladium.* Care must be taken not to get fingerprints or dust particles on the surface of the stubs, as EDXRA will detect significant amounts of potassium, chlorine, and other elements. Therefore, samples are stored in dust-free plastic containers and all stubs are handled with tweezers.

ANALYTICAL METHODOLOGY

The analytical procedure for prepared samples is constrained by time available on the SEM, the time the EDXRA takes to scan an individual particle or field of particles, and the cost of the analysis. Since the object of this study was to characterize the particulate samples by morphology and chemistry relationships, the following conditions were set:

- A maximum time limit of 1 hour was set for SEM analysis.
- An initial low magnification scan at roughly 75X was made to determine if the particulate loading was sufficient.
- A 200-second EDXR analysis of the entire field of view at approximately 75X was made to provide an overall chemical makeup and to determine gross similarities or dissimilarities among samples. A photograph of the X-ray spectrum of this scan was taken. Figures C-1 through C-5 present the overall chemical/spectral analyses for the five FBC fly ash samples.
- Approximately 25 particles from each sample were selected for morphological and chemical determination at a magnification of 750-1500X. The selection of particles was randomly performed unless a sample provided an abundance of an unusual

*Peaks noted for gold and palladium are due to the use of these materials as coating agents in slide preparation and not to their natural occurrence as fly ash constituents.

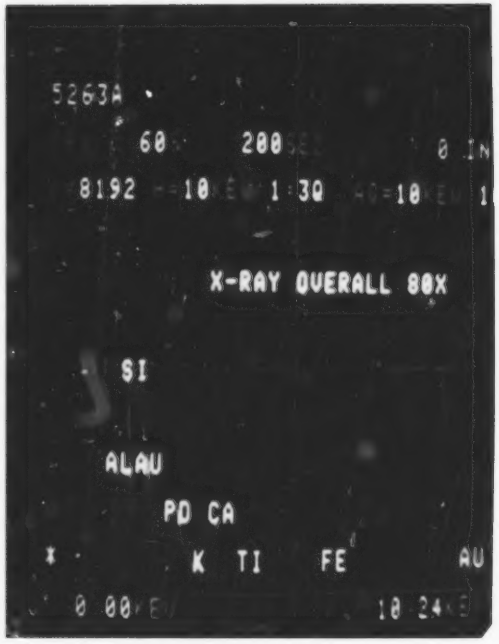

Figure C-1. Chemical/spectral analysis of fly ash Sample A (Alliance).

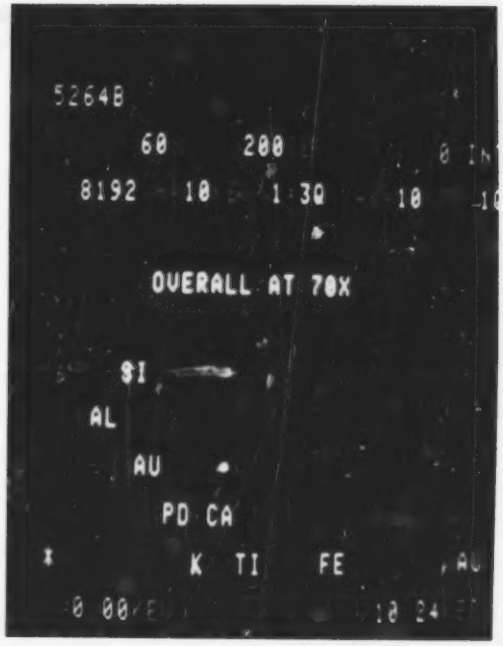

Figure C-2. Chemical/spectral analysis of fly ash Sample B (SATR).

Figure C-3. Chemical/spectral analysis of fly ash Sample C (FluiDyne without recycle).

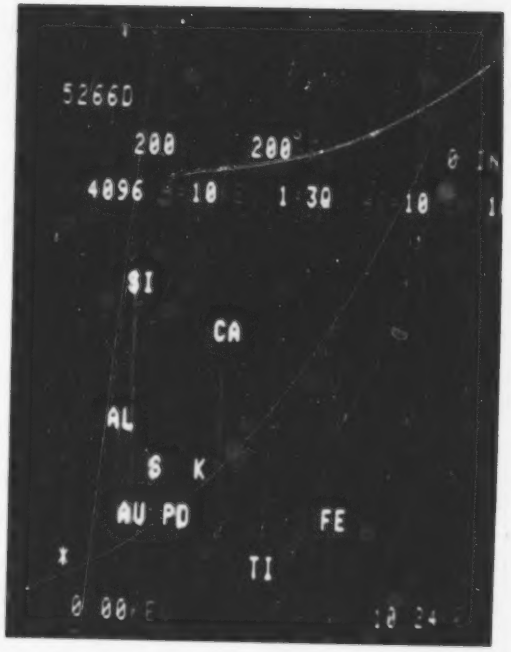

Figure C-4. Chemical/spectral analysis of fly ash Sample D (FluiDyne with recycle).

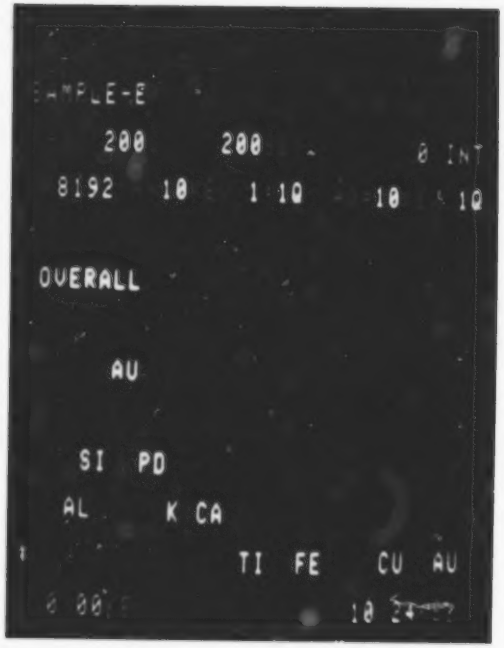

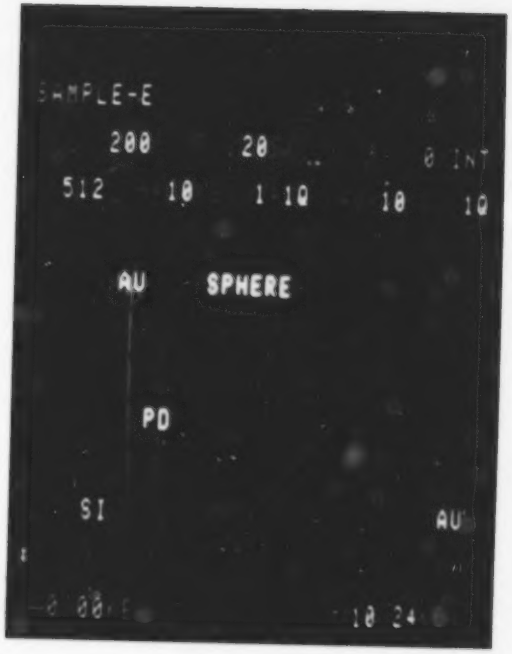

Figure C-5. Chemical/spectral analysis of fly ash Sample E (Georgetown).

morphology. The actual number of particles analyzed was limited by the 1-hour time constraint.

- All data, such as each element detected, relative abundance as determined by peak height on the spectrum, and morphology and/or texture, were recorded. These results are presented in Tables C-1 through C-5.

PRESENTATION OF RESULTS

As mentioned, Tables C-1 through C-5 summarize the morphology and elemental composition of the AFBC fly ash samples described earlier in this report. An examination of the morphology of these particulate samples suggests highly variable particle shape and size properties for FBC fly ash, as contrasted to the more uniformly spherical nature of fly ash produced by conventional combustion, discussed in the main text and shown in Figures 1 and 2.

EDXRA results show no apparent striking differences in chemical composition between the FBC fly ash samples and fly ash produced by conventional combustion. All AFBC samples are relatively high in Al_2O_3 and SiO_2 as is the case with most conventionally produced fly ash. The relatively high CaO contents observed may result from the limestone that is injected into the fluidized-bed for SO_2 control. Additionally, lignite and subbituminous coal ashes have relatively high percentages of CaO.[1] All of the AFBC fly ash samples exhibited higher than normal (>5 percent) carbon contents, with extremely high values noted for two of the samples (as high as 46 percent in one case). As mentioned in the main text, this condition may lead to blinding of fabric filter bags and possible ignition in electrostatic precipitators.

TABLE C-1. MORPHOLOGICAL CHARACTERIZATION AND ELEMENTAL COMPOSITION OF FLY ASH SAMPLE A (ALLIANCE)

		Elements detected[+]							
	Morphology*	Na	Al	Si	S	K	Ca	Ti	Fe
1	Spherical		X_m	X_m		X	X		X
2	Spherical		X	X_m			X		
3	Spherical		X_m	X_m		X	X		
4	Spherical		X_m	X_m			X		
5	Spherical	X_t	X_m	X_m		X	X	X_t	X
6	Spherical		X	X					X_m
7	Spherical		X_m	X_m		X	X_m	X_t	X
8	Angular								X_m
9	Angular		X_t	X_t			X_t		X_m
10	Angular		X_t	X_t		X_t	X_t		
11	Angular		X_t	X_t	X_t				
12	Angular		X_t	X_t					
13	Platy		X_t	X_t					
14	Subangular		X	X_m	X	X	X_m		X
15	Angular		X	X	X_m		X_m		X
16	Angular		X	X_m	X		X_m		
17	Angular		X	X	X_m		X_m		
18	Angular		X_m	X_m		X	X	X_t	
19	Platy		X_m	X_m		X	X		
20	Tabular		X_m	X_m		X	X		X_t
21	Angular		X_m	X_m		X	X		
22	Tabular		X_m	X_m		X	X	X_t	X
23	Subangular		X	X_m			X		
24	Platy		X_m	X_m		X			
25	Blocky		X	X					

*Definition of terms used to describe particle morphology in Tables C-1 through C-5:

- Angular: Particles having sharp corners, a radius of curvature equal to zero, and nonabraded surfaces.
- Subangular: Particles whose corners are not sharp but have a small radius of curvature, and most of the surfaces are not abraded.
- Platy: Particles having a plate-like appearance.
- Tabular: Flat, elongated particles with defined angles and parallel faces.
- Blocky: Particles having a block-like appearance.
- Lacy: Thin, platy particles having a porous appearance.
- Granular: Irregularly shaped (often agglomerated) particles whose individual grains interlock.
- Lathlike: Long, thin cylindrical particles.

[+]Elements detected:

- X ≡ Detectable peak
- X_m ≡ Major peak
- X_t ≡ Trace peak

TABLE C-2. MORPHOLOGICAL CHARACTERIZATION AND ELEMENTAL COMPOSITION OF FLY ASH SAMPLE B (SATR)*

		Elements detected							
	Morphology	Na	Al	Si	S	K	Ca	Ti	Fe
1	Spherical		X_m	X_m			X_m		
2	Spherical		X	X_m	X		X_m		X_t
3	Spherical		X_m	X_m		X	X		
4	Spherical		X_m	X_m	X_t	X_t	X_m		X
5	Spherical		X_m	X_m	X		X		X
6	Spherical		X_m	X_m	X	X_t	X	X_t	X_t
7	Spherical		X_m	X_m					
8	Spherical		X_m	X_m	X	X	X_m		X_t
9	Angular-Platy		X_t	X_t					
10	Angular		X_m	X_m	X	X	X		
11	Subangular		X	X_m	X		X_m		X_m
12	Subangular		X_m	X_m	X		X_m		
13	Angular		X	X_m	X_m		X_m		
14	Subangular			X	X_m		X_m		
15	Angular			X	X_m		X_m		
16	Platy		X	X_m	X_t	X_t	X_t		
17	Angular		X	X_m	X		X		
18	Subangular		X_m	X_m	X_m		X_m		
19	Subangular		X	X_m		X	X		
20	Angular-Platy		X_m	X_m		X			
21	Angular		X_m	X_m		X_t	X		X_t
22	Angular		X_m	X_m		X	X_m		
23	Angular		X	X_m			X		
24	Angular		X_m	X_m			X		
25	Angular	X	X	X_m					

*Refer to footnotes on Table C-1.

TABLE C-3. MORPHOLOGICAL CHARACTERIZATION AND ELEMENTAL COMPOSITION OF FLY ASH SAMPLE C (FLUIDYNE WITHOUT RECYCLE)*

		Elements detected							
	Morphology	Al	Si	S	K	Ca	Ti	Fe	Mg
1	Spherical	X	X_m	X_m	X_t	X_m		X_t	
2	Spherical	X	X_m			X_m		X	
3	Spherical	X	X_m		X	X_m		X	
4	Spherical	X_m	X_m		X	X	X_t	X_t	
5	Angular (Lacy)	X	X_m	X_m	X_t	X_m		X	
6	Subangular (Lacy)	X_t	X_t	X_t		X_t			
7	Angular (Lacy)	X_t	X_t	X_t		X_t			
8	Subangular	X_m	X_m		X	X			
9	Angular	X_m	X_m		X			X	
10	Subangular	X_m	X_m		X	X			
11	Angular	X_t	X	X_m		X_m		X_t	X
12	Angular-Platy	X_m	X_m		X_t	X_t		X_t	
13	Subangular	X_m	X_m		X_m	X_t			
14	Angular	X_t	X	X_m		X_m			
15	Angular			X_m		X_m			
16	Angular	X_t	X	X_m		X_m		X_t	X_t
17	Angular	X_t	X_t	X_m		X_m			
18	Angular	X_t	X_t	X_m		X_m			
19	Angular	X_t	X_t	X_m		X_m			
20	Angular	X_t	X_t	X_m		X_m			
21	Tabular			X_m		X_m			
22	Angular		X_t					X_m	
23	Angular	X_t	X_t			X_t		X_m	
24	Platy	X	X_m					X_t	X_m
25	Lathlike	X_m	X_m						

*Refer to footnotes on Table C-1.

TABLE C-4. MORPHOLOGICAL CHARACTERIZATION AND ELEMENTAL COMPOSITION OF FLY ASH SAMPLE D (FLUIDYNE WITH RECYCLE)*

		Elements detected							
	Morphology	Al	Si	S	K	Ca	Ti	Fe	Mg
1	Spherical		X_m			X_m			
2	Spherical	X_m	X_m		X	X			
3	Spherical	X	X			X_m		X_m	
4	Spherical	X_t	X_t					X_m	
5	Spherical	X_t	X_m			X			
6	Spherical		X_m						
7	Spherical	X_m	X_m		X	X		X	
8	Spherical	X_t	X			X			
9	Spherical	X	X_m		X	X_m		X_m	
10	Angular (Lacy)			X_m					
11	Angular (Lacy)	X_m	X_m		X	X			
12	Angular (Lacy)	X_t	X_t	X_t					
13	Angular	X	X	X_m	X	X			
14	Angular	X_t	X	X_m		X_m			
15	Angular	X	X_m	X_m		X_m		X	X_t
16	Angular	X	X	X_m		X_m			
17	Angular	X	X	X_m		X_m		X_t	
18	Angular	X_t	X_t	X_m		X_m		X	
19	Angular	X	X_m	X	X	X_m		X	X_t
20	Angular	X_t	X_t	X_m		X_m			
21	Blocky		X_t	X_m		X_m			
22	Angular	X_t	X_t	X_m		X_m			
23	Tabular		X_t	X_m		X_m			
24	Angular	X	X_m			X_m			
25	Angular	X_m	X_m		X	X_m	X	X_m	
26	Platy	X	X		X	X	X	X	
27	Lathlike	X	X			X_m	X	X	
28	Angular	X_m	X_m		X_m	X_m		X	
29	Angular	X	X			X			
30	Lathlike	X_m	X_m		X	X			
31	Platy	X_m	X_m		X_m			X	
32	Angular	X_m	X_m		X	X			
33	Angular		X			X_m		X	
34	Platy	X_m	X_m		X_m	X_m			
35	Fibrous	X_m	X_m			X			
36	Granular		X_t			X_t		X_m	

*Refer to footnotes on Table C-1.

TABLE C-5. MORPHOLOGICAL CHARACTERIZATION AND ELEMENTAL COMPOSITION OF FLY ASH SAMPLE E (GEORGETOWN)*

	Morphology	Elements detected				
		Al	Si	K	Ca	Fe
1	Fractured Sphere	X_m	X_m	X	X	X
2	Irregular (Carb.)†		X_t			
3	Blocky-Angular	X_m	X_m	X	X	X
4	Angular (Carb.)	X	X			
5	Platy (Carb.)‡					
6	Granular	X_m	X_m		X	X
7	Subangular	X_m	X_m	X	X	X
8	Subangular	X_m	X_m			
9	Granular (Carb.)‡					
10	Lacy-irregular (Carb.)‡					
11	Angular	X_m	X_m			
12	Spherical (Carb.)		X_m			
13	Granular	X	X_m		X	X
14	Platy	X_m	X_m			
15	Spherical	X_m	X_m	X	X_m	
16	Subangular (Carb.)		X_t			
17	Spherical (Carb.)		X_t			
18	Spherical (Carb.)‡					
19	Spherical (Carb.)‡					
20	Subangular (Carb.)		X_t			

*Refer to footnotes on Table C-1.

†(Carb.) represents carbonaceous material.

‡No elements detected.

REFERENCES FOR APPENDIX C

1. Abernathy, R. F., M. J. Peterson, and F. H. Gibson. Major Ash Constituents in U.S. Coals. U.S. Bureau of Mines Report No. 7240. 1969.